

# UC Irvine

## UC Irvine Electronic Theses and Dissertations

### Title

Study of Polymer-filler composites Based High Performance Diffuse Optical Reflectors for Optoelectronic Device Applications

### Permalink

<https://escholarship.org/uc/item/27h0b09k>

### Author

Shao, Yue

### Publication Date

2016

Peer reviewed|Thesis/dissertation

UNIVERSITY OF CALIFORNIA,  
IRVINE

Study of Polymer-filler Composites Based High Performance Diffuse Optical Reflectors for  
Optoelectronic Device Applications

DISSERTATION

submitted in partial satisfaction of the requirements  
for the degree of

DOCTOR OF PHILOSOPHY

in Materials Science and Engineering

by

Yue Shao

Dissertation Committee:  
Professor Frank G. Shi, Chair  
Professor James C. Earthman  
Professor Mikael Nilsson

2016

Chapter 2 © 2015 Optical Society of America  
Chapter 3 © 2016 Optical Society of America  
All other chapters © 2016 Yue Shao

## TABLE OF CONTENTS

	Page
LIST OF FIGURES	iii
LIST OF TABLES	vii
ACKNOWLEDGMENTS	viii
CURRICULUM VITAE	ix
ABSTRACT OF THE DISSERTATION	x
CHAPTER 1: Background and introduction	1
CHAPTER 2: Study of optimal filler size for high performance polymer-filler composite optical reflectors	15
CHAPTER 3: Exploring the Critical thickness for maximum reflectance of optical reflectors based on polymer-filler composites	34
CHAPTER 4: Effect of fillers on silicone-based diffuse reflective films for LCD backlight units	54
CHAPTER 5: Radiation Cooling Enabled by Novel Polymer Composite Coating: Filler Size Effect	74
CHAPTER 6: Dual-functional composites for high optical diffusive reflectance and passive cooling	88
CHAPTER 7: Summary and Conclusions	100

## LIST OF FIGURES

		Page
Figure 1.1	The schematic cross-sectional view of a LED package	3
Figure 1.2	Projected cost track for a LED-based A-19 60W replacement lamp	4
Figure 1.3	Different types of reflectors including metallic reflector, distributed Bragg reflector (DBR), hybrid reflector, total internal reflector (TIR), and omni-dirrectional reflector (ODR)	6
Figure 1.4	Scattering of light by white paint film	7
Figure 1.5	Typical white LED flux vs junction temperature	9
Figure 1.6	Example of radiation: (a). The sun heating the earth, (b). the radiant heat transfer	10
Figure 1.7	Heat transfer in a LED thermal system. Heat transfer from die to the surrounding environment by conduction, convection and radiation	11
Figure 2.1	Schematic of light scattering in silicone-filler composite reflectors	18
Figure 2.2	The prediction of reflectance as a function of filler size-wavelength ratio for composite reflectors with different filler-matrix refractive index ratio ( $RIR = n_{\text{filler}}/n_{\text{matrix}}$ ) at wavelength of 450nm.	20
Figure 2.3	The prediction of critical filler size as a function of RIR (a). for polymer-based reflectors at different wavelength and (b). for silicone-based reflectors at wavelength of 450nm. The symbols indicate the measured optimized filler size with different fillers (left: $Al_2O_3$ , right: $TiO_2$ ) and the line shows the calculated optimized filler size based on model.	21
Figure 2.4	The Thinky centrifuge mixer for silicone matrix and filler mixing	24
Figure 2.5	The vacuum oven for degassing (Fisher scientific, Model 280A)	24
Figure 2.6	The stainless steel molds and molded reflector samples	26
Figure 2.7	Normalized reflectance vs. particle size for 3mm thick (a) $Al_2O_3$ -silicone composites and (b) $TiO_2$ -silicone composites at wavelength of 450nm with 0.1 filler volume fraction. For better comparison, reflectance is normalized by setting the highest value as 1. The circles indicate the measured reflectance and the lines show the calculated	

	reflectance based on model.	27
Figure 3.1	The schematic cross-sectional view of a LED package	36
Figure 3.2	The BYK thin film applicator for reflective films preparation	38
Figure 3.3	The coating thickness gauge for thickness measurement (CEM Model DT-156)	38
Figure 3.4	The prediction of reflectance as a function of thickness of reflector for different back reflection from substrate	42
Figure 3.5	The prediction of reflectance as a function of reflector thickness of reflector for different filler volume fraction	42
Figure 3.6	The prediction of reflectance as a function of volume fraction of reflector	43
Figure 3.7	Reflectance change of (a) BN-silicone coatings and (b) ZnO-silicone coatings on Cu substrate ( $R' = 0.07$ ) and Al substrate ( $R' = 0.78$ ) at wavelength of 450nm. The filler volume fraction is 0.1. The symbols indicate the measured reflectance with different thickness ( $x$ ) and the lines show the theoretical reflectance based on model	44
Figure 3.8	Reflectance vs. reflector thickness for (a) BN-silicone coatings and (b) ZnO-silicone coatings on Cu substrate ( $R' = 0.07$ ) at wavelength of 450nm. The symbols indicate the measured reflectance with different filler volume fraction ( $f$ ) and the lines show the theoretical reflectance based on model	46
Figure 3.9	Reflectance vs. filler volume fraction for (a) BN-silicone coatings and (b) ZnO-silicone coatings on Cu substrates at wavelength of 450nm with various thickness. The symbols indicate the measured reflectance at different thickness ( $x$ ) and the lines show the calculated reflectance based on model	48
Figure 3.10	Reflectance of (a) 110 $\mu\text{m}$ thick BN-silicone coatings and (b) 125 $\mu\text{m}$ thick ZnO-silicone coatings on Cu substrate and Al substrate. The filler volume fraction is 0.1. The symbols indicate the measured reflectance at different wavelength and the lines show the theoretical reflectance based on model	50
Figure 4.1	Structures of (upper) direct-type backlight and (lower) edge-type backlight	56
Figure 4.2	Vulcan programmable furnace for high temperature thermal aging	59

Figure 4.3	ChemKorea Temperature and humidity chamber used for high temperature/ humidity test	60
Figure 4.4	Reflectance vs. reflector thickness for (a) Al <sub>2</sub> O <sub>3</sub> -silicone composites, (b) TiO <sub>2</sub> -silicone composites and (c) ZnO-silicone composites at wavelength of 450nm with various thickness	62
Figure 4.5	Reflectance loss of silicone reflective films filled with Al <sub>2</sub> O <sub>3</sub> , TiO <sub>2</sub> , BN, ZnO and SiO <sub>2</sub> under 150°C aging for 500 hours at (a) 450nm, (b) 550nm and (c) 630nm wavelength	65
Figure 4.6	Reflectance loss of silicone reflective films filled with Al <sub>2</sub> O <sub>3</sub> , TiO <sub>2</sub> , BN, ZnO and SiO <sub>2</sub> under high temperature at 85°C and humidity at 85% RH for 500 hours at (a) 450nm, (b) 550nm and (c) 630nm wavelength	67
Figure 4.7	Reflectance loss of commercial EMC and lab-made SMC under (a) 994718 W/m <sup>2</sup> blue radiation + 150°C aging for 1080 hours and (b) UV radiation + 150°C aging for 24 hours	69
Figure 5.1	SEM images of Al <sub>2</sub> O <sub>3</sub> fillers at size of (a) 40nm, (b) 100nm, (c) 1 micron and (d) 10microns	76
Figure 5.2	Schematic drawings of heating system	77
Figure 5.3	Board temperature of (a) Al <sub>2</sub> O <sub>3</sub> , (b) TiO <sub>2</sub> and (c) ZnO composites coatings as a function of filler size. The filler volume fraction is 0.1 and the coating thickness is 70±5 microns. The input power is fixed at 9 Watts.	79
Figure 5.4	Normalized emissivity of graphite particles at different temperatures. The emissivity of the particle increases as the size increases.	82
Figure 5.5	(a) Schematic drawing of polymer-filler composites consisting of polymer matrix, interphase region and filler. (b) Illustration of the change of surface-to-volume ratio as a function of filler size. The surface to volume ratio for a filler is defined as the proportion of surface atoms to total atoms	82
Figure 5.6	Reduction of board temperature of Al <sub>2</sub> O <sub>3</sub> composites coatings at input power of 9 W and 25 W. The filler volume fraction is 0.1 and the coating thickness is 70±5 microns	83
Figure 5.7	Illustrates the effect of coating thickness on the cooling effect of Al <sub>2</sub> O <sub>3</sub> composite coating at input power of 25 W. The filler used is	

	1 $\mu\text{m}$ $\text{Al}_2\text{O}_3$ powders and the filler volume fraction is 0.1	84
Figure 6.1	Technological process for samples preparation	91
Figure 6.2	Cross-sectional and top-view structure of LED unit consist of a LED package mounted on a coated PCB. Red spot is the measurement position for LED emitter temperature	92
Figure 6.3	Temperature vs. time for LED unit incorporated with ZnO-silicone composite coatings with different filler volume fraction	93
Figure 6.4	Temperature reduction of LED unit consist of LED emitter and PCB coated with (a) ZnO, (b) $\text{TiO}_2$ and (c) BN filled silicone composites vs. light reflectance of silicone composite coatings. The filler volume fractions are 0.025, 0.05, 0.1, 0.2 and 0.3. The coating thickness is $50\pm 5$ microns. The power of LED is 10 Watts.	93



## LIST OF TABLES

		Page
Table 1.1	Comparison between LED and traditional light sources	2
Table 1.2	Comparison between silicone resin and other polymers	8
Table 3.1	Properties of materials used for samples	37
Table 4.1	Properties of materials used for reflectors	57
Table 6.1	Properties of materials used for samples	90

## ACKNOWLEDGMENTS

I would like to express the deepest appreciation to my committee chair, Professor Frank G. Shi, who has the attitude and the substance of a genius: he continually and convincingly conveyed a spirit of adventure in regard to research, and an excitement in regard to instruction. Without his guidance and persistent help this dissertation would not have been possible.

I would like to thank my committee members, Professor James C. Earthman and Professor Mikael Nilsson, for their time and efforts in serving as my dissertation committee member, and their valuable suggestions on my work.

In addition, a thank you to Dr. Jiun-Pyng You, Dr. Yeong-Her Lin, Dr. Bohan Yan and Dr. Yun Shuai. As my seniors they provided invaluable help and suggestions on my research, from experiment trainings to technical discussions.

I also thank my junior colleague, Linguan Huang and Gunwoo Kim, for their help on related experiments.

Special thanks to Yi-San Chang-Yen, Grace Chau, Beatrice Mei, Janine Le and Steve Weinstock at Materials Science Department for helping me through my works.

Last but not least, I would like to thank my family for their unlimited support.

# CURRICULUM VITAE

## Yue Shao

- 2005-2009 B. S. in Materials Science and Engineering, Donghua University, China
- 2009-2010 M. S. in Materials Science and Engineering, University of California, Irvine
- 2012-2016 Ph. D. in Materials Science and Engineering, University of California, Irvine

## FIELD OF STUDY

Optoelectronic Packaging Materials and Technology

## PUBLICATIONS

Yue Shao, Frank G. Shi. " Radiation Cooling Enabled by Novel Polymer Composite Coating: Filler Size Effect " (2016, Submitted)

Yue Shao, Frank G. Shi. " Effect of fillers on silicone-based diffuse reflective films for LCD Backlight Units" (2016, Submitted)

Yue Shao, Frank G. Shi. "Exploring the critical thickness for maximum reflectance of optical reflectors based on polymer-filler composites" Optical Materials Express, Vol. 6 Issue 6, pp. 1106-1113, 2016.

Yue Shao, Yu-chou Shih, Gunwoo Kim and Frank G. Shi. "Study of optimal filler size for high performance polymer-filler composite optical reflectors" Optical Materials Express, Vol. 5 Issue 2, pp. 423-429, 2015.

Yue Shao, Yu-chou Shih, Gunwoo Kim and Frank G. Shi. "Filler size dependence of optical reflectance for polymeric-filler reflectors" Presented at 65<sup>th</sup> IEEE Electronic Components and Technology Conference, 2015.

Yue Shao, Yu-Chou Shih and Frank G. Shi. "Reliability potential of silicone molding compounds for LED application." Presented at 47<sup>th</sup> International Symposium on Microelectronics, 2014.

Yu-Chou Shih, Yue Shao, Yeong-Her Lin and Frank G. Shi. "Nano-sized glass frits with surface treatment for silicon solar cells" 2013 IEEE International Symposium on Advanced Packaging Materials, pp. 290-296

# **ABSTRACT OF THE DISSERTATION**

Study of Polymer-filler Composites Based High Performance Diffuse Optical Reflectors for Optoelectronic Device Applications

By

Yue Shao

Doctor of Philosophy in Materials Science and Engineering

University of California, Irvine, 2016

Professor Frank G. Shi, Chair

The packaging materials are critical for optoelectronic device packaging in terms of optical and thermal performance. Continuous innovation and improvement of packaging materials have been introduced to improve the overall efficiency of LEDs, but there are still some critical issues need to be addressed for their application in general lighting and LCD backlight displays. In this work, high performance and cost-effective silicone-filler composites are investigated and introduced to LEDs and LCD backlight units to enhance their optical and thermal management.

The first part of the work is development of reflector packaging materials. The reflectance of polymer-filler reflectors was optimized by controlling filler particle size, filler volume fraction and thickness of reflectors. A simple analytical model was developed to investigate the critical parameters of inorganic fillers required to obtain the highest reflectance, which is expected to accelerate the design and optimization of polymer-filler composite reflectors. Our results demonstrate for the first time that for inorganic fillers, the effect of filler size on reflectance is non-monotonic, and a critical filler size ranging from one submicron to several microns provides

the maximum reflectance. The existence of a critical thickness at which the optical reflectance of a polymer-filler composite reaches its maximum value is demonstrated.

In the second part of this work, the apparent radiation cooling effect of silicone-based composite coatings was investigated for its dependence on coating thickness and filler size. It is established, contrary to prior reports, that the effective passive radiation cooling does not exhibit a significant filler size dependence. We found the apparent cooling effect is filler type dependent and the optimal thickness is around 70  $\mu\text{m}$  regardless of filler type.

In the third part of this work, dual-functional polymer-filler composites with high optical diffusive reflectance and passive cooling ability is investigated for optoelectronic device applications. It was demonstrated the addition of inorganic fillers to a volume fraction higher than 0.2 can effectively improve the apparent cooling effect and light reflectance of silicone composites. The new materials we developed can be used as diffuse reflector to provide better overall optical aesthetics for displays. Meanwhile, it can be used as passive cooling coatings in advanced general LED lighting, LCD display backlighting, solar cells and other energy related applications.

# **CHAPTER 1:**

## **BACKGROUND AND INTRODUCTION**

### **1.1 Background**

The demand of energy related devices including light-emitting diodes (LEDs) and solar cells has been expanding in the past decades due to the global trends toward more environmental friendly technology. LEDs are optoelectronic devices which produce minority carriers injected using p-n junctions in semiconductors and emit light by recombination of the minority carriers. LEDs have been widely employed as a replacement for conventional light sources in various industrial fields concerned with every saving, such as general lighting and display backlights [1-3]. Automotive and smart lighting are two recently developed markets for LED applications. Compared with traditional light sources, LEDs have advantages such as: high conversion efficiency, long lifetime without burning out, reduced physical size, rapid response time, resistance to vibration, repeated switching and lack of toxic substances regulated by environmental regulations.

Table 1.1 Comparison between LED and traditional light sources

Lamp type	Luminous efficacy (lm/W)	Efficacy limits (lm/W)	Initial cost per lumen (\$/lm)	Maximum lifetime (hours)	Warm-up time (min)	Power factor	Dimmable	Frequent switching acceptable
Oil lamp	0.1	0.1	N/A	N/A	N/A	N/A	N/A	N/A
Incandescent	8 – 14	50	0.001	2000	N/A	1	Y	Y
Halogen	15 – 25	50	0.005	5,000	N/A	1	Y	Y
Metal halide discharge	60 – 130	230	0.005	20,000	2 – 5	0.85 - 0.99	N	N
Linear fluorescent	45 – 100	120	0.002	60,000	5 – 20	~ 0.4 – 0.7	N	N
Compact fluorescent	50 – 70	120	0.006	15,000	3 – 15	~ 0.3 – 0.7	N	N
LED	50 – 100	240	0.04	100,000	N/A	up to 1	Y	Y
Organic LED	18 – 50	240	unknown	10,000	N/A	unknown	Y	Y

(Source: A Global Village)

Figure 1.1 shows the schematic drawing of the cross-sectional view of a monochromatic blue LED package with encapsulant. A typical manufacturing process of LED package via surface mount technology includes attaching a LED chip with die attach adhesive (DAA), bonding the chip on leadframe with gold wires, sealing the chip by encapsulant compound, mounting the leadframe on a printed circuit board (PCB), and then attaching the resulting LED unit on a heat sink for heat dissipation. The packaging design and packaging materials play very important roles in determining LEDs optical performance. There are continuously advancements in LED packaging materials and technologies, including the addition of reflective layers, novel chip surface optical structures for light extraction, multi-layered phosphor for white LEDs and new encapsulation materials with improved thermal and radiation resistance.

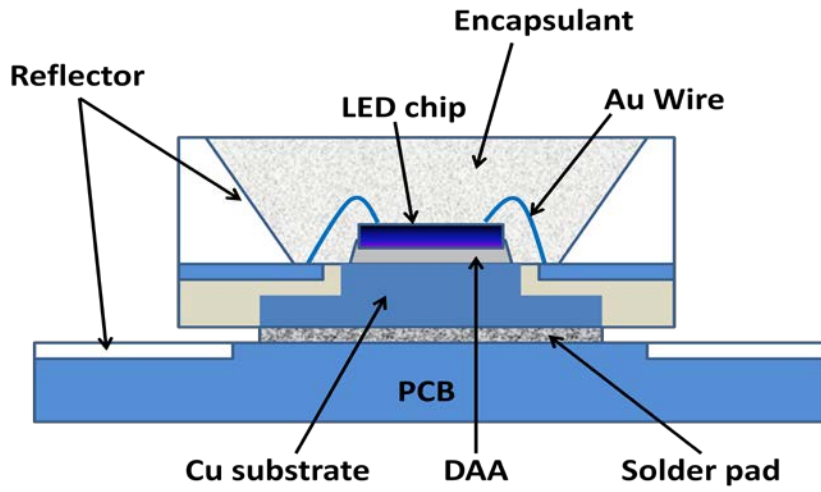


Fig. 1.1. The schematic cross-sectional view of a LED package.



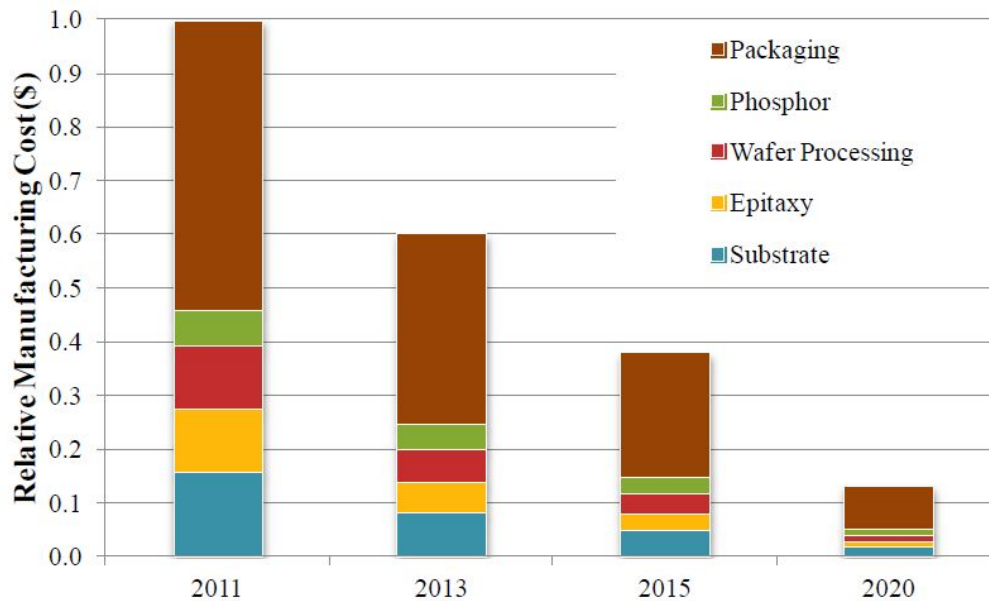


Fig. 1.2. Projected cost track for a LED-based A-19 60W replacement lamp.

(source: data provided by 2011 Manufacturing Roundtable attendees)

Numerous advanced packaging technologies have been introduced into LEDs devices to improve the overall efficiency, but critical issues including optical management and thermal management still need to be addressed for their application in general lighting and LCD backlight displays.

## 1.2 Optical management

Currently, two main fields of LED applications are general lighting and backlight units. Backlight units are required for many consumer electronics, such as thin-film-transistor liquid-crystal display (TFT-LCD) and mobile phones. LCD backlight provides better optical performance and less energy consumption than the conventional cold cathode fluorescent light (CCFL). LCD backlight is also more compact in size, lighter, and last longer than CCFL.

Optical reflective materials are key components to the development of high performance lighting modules, display backlighting modules, as well as solar cells [4-5]. The reflectors used in LEDs and backlight units have a significant impact on their brightness, uniformity, color and stability [6]. The light trapping in the electronics package is one of the major cause to the light loss and should be minimized to attend the maximum efficiency. An ideal optical reflector requires high light reflectivity in order to reduce the loss of exiting light for achieving high light extraction efficiency with low energy consumption. Long operational lifetime, low manufacturing cost (see Fig.1.2) are also important requirements for development of optical reflector for LEDs and solar cells applications.

The rapid commercialization of LED lighting and solar cell technology requires the development of advanced reflector materials to perform multi-functions. A new set of requirements for reflectors are high light reflectivity, light guidance, light spectrum filtering (UV/IR absorption), mechanical protection for light source, long operation lifetime and cost affectivity. There are still much rooms for the improvement of reflector materials. High performance optical reflectors for industrial LEDs and solar cells are commonly accomplished by metallic mirrors ( i.e. silver and aluminum mirrors), conventional dielectric mirrors (i.e. distributed Brag reflectors and all-dielectric omni-directional mirrors) and diffusive dielectric reflectors. The comparison of above-mentioned reflectors is shown in figure 1.3. Recently, diffusive dielectric reflectors such as polymer-filler composite reflectors have gained great attention as an alternative candidate because of their capability of high reflectance over a broad spectral range and their potential for low cost. In addition, they can improve uniformity of light distribution, eliminating “dots” and glare for better overall optical aesthetics for LEDs lighting applications.

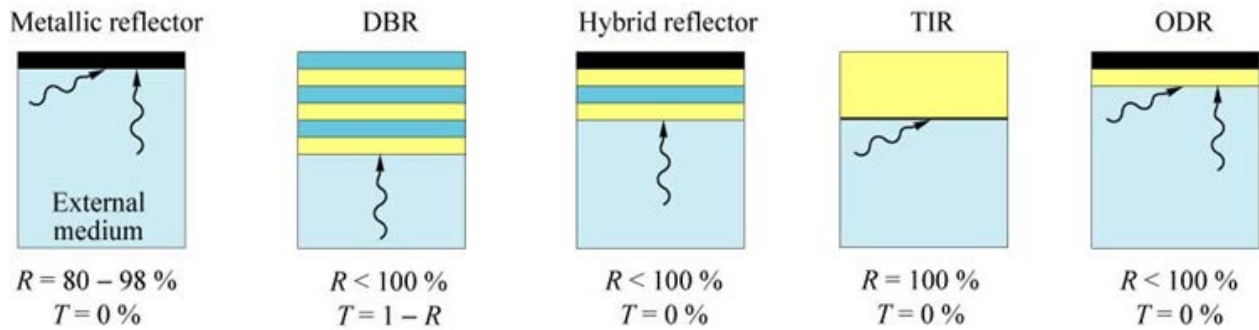


Fig. 1.3. Different types of reflectors including metallic reflector, distributed Bragg reflector (DBR), hybrid reflector, total internal reflector (TIR), and omni-directional reflector (ODR).

Also given are angles of incidence for high reflectivity and typical reflectances and transmittances.

Figure 1.4 shows the light scattering by white paint containing white filler particles. For polymer-filler composites reflectors, the interaction between the filler particles and matrices plays a key role in the optical properties. Key parameters including particle size, the refractive index difference between particles and matrix and the reflectivity of fillers in the visible region, are crucial and important for resulting optical reflectance.

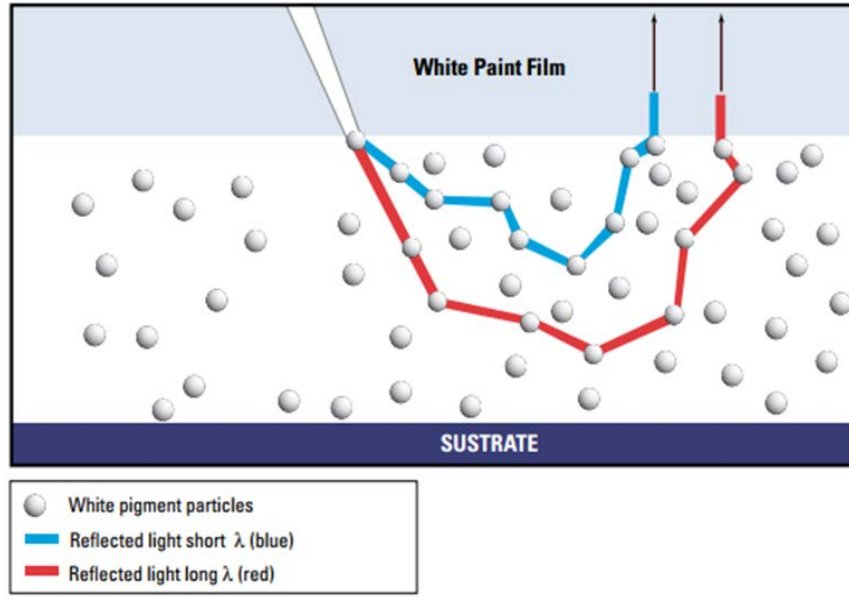


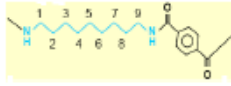

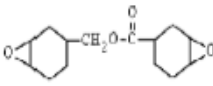

Fig. 1.4. Scattering of light by white paint film.

(Source: Dupont)

Common materials used for LED leadframe reflectors are polyphthalamide (PPA), polycyclohexylenedimethylene terephthalate (PCT) and epoxy mounting compound (EMC). PPA shows high reflectance (>95%) in visible wavelength spectrum, but its resistance of heat and radiation is very limited so is only applicable for LEDs with power lower than 0.5 watts. EMC has lower initial reflectance than PPA, but it shows better resistance to heat and radiation and is gradually replacing PPA for mid power LEDs. Silicone molding compound (SMC) is the latest technology in packaging material for high power LEDs because of its high initial reflectance, good chemical stability and superior thermal and UV resistance, as presented in Table.1.2. SMC also exhibits durability, flexibility, good resistance to discoloration over time and excellent adhesion with silicone encapsulants. There is a great interest in the development of cost-effective and high performance silicone-based packaging materials in order to decrease the price-performance ratio for optical and photonic devices.

Table. 1.2. Comparison between silicone resin and other polymers.

(Source: Shin-Etsu)

	Thermoplastic		Thermosetting	
	6T & 9T	PCT	Epoxy	Silicone
Feature	9T	PCT	Epoxy	Silicone
Chemical structure				
Advantage	<ul style="list-style-type: none"> <li>• High white-ness <math>\geq 95\%</math></li> <li>• Good mold-ability</li> <li>• Lower material cost (\$15 /KG)</li> </ul>	<ul style="list-style-type: none"> <li>• Good resistance to heat and light damage</li> <li>• Good reliability</li> </ul>	<ul style="list-style-type: none"> <li>• Excellent resistance to heat and light damage</li> <li>• Excellent reliability</li> <li>• Initial white-ness ~ 94.8%</li> </ul>	<ul style="list-style-type: none"> <li>• Excellent resistance to heat and light damage</li> <li>• Excellent reliability</li> <li>• Good adhesion with Silicone</li> <li>• High white-ness ~97%</li> </ul>
Dis-advantage	<ul style="list-style-type: none"> <li>• Poor resistance to heat and light damage</li> </ul>	<ul style="list-style-type: none"> <li>• Low White-ness ~93.9%</li> <li>• Slightly high material cost ( ~ \$22/KG)</li> <li>• Poor mold-ability</li> </ul>	<ul style="list-style-type: none"> <li>• High material cost ( ~ \$170/KG)</li> <li>• Transfer molding</li> </ul>	<ul style="list-style-type: none"> <li>• Very high material cost ( ~ \$500/KG )</li> <li>• Transfer molding</li> </ul>
Operation power	Under 0.5 Watts PKG	0.4~0.7Watts	0.4~1.0 Watts	> 1.0 Watts

### 1.3 Thermal management

With the development of optoelectronic devices such as LEDs, LCD display backlight and solar cells towards thinner and higher power, packaging materials are facing the challenges of withstand with higher heat flux density [8-9]. Optoelectronic devices can generate a significant amount of waste heat during the operation. For example, high-efficiency LEDs only convert 30% of electric power to light, while the remaining 70% is transferred to heat [10]. In high power LEDs, heat is conducted from the chip to the printed circuit board (PCB) and then dissipated to surrounding air. As the waste heat accumulates, the high temperature of printed circuit board and the electronic elements result in a shorter lifetime, lower luminance flux or

even failure of the entire electronic device. More efforts are needed for people to research and develop new method for electronic system cooling.

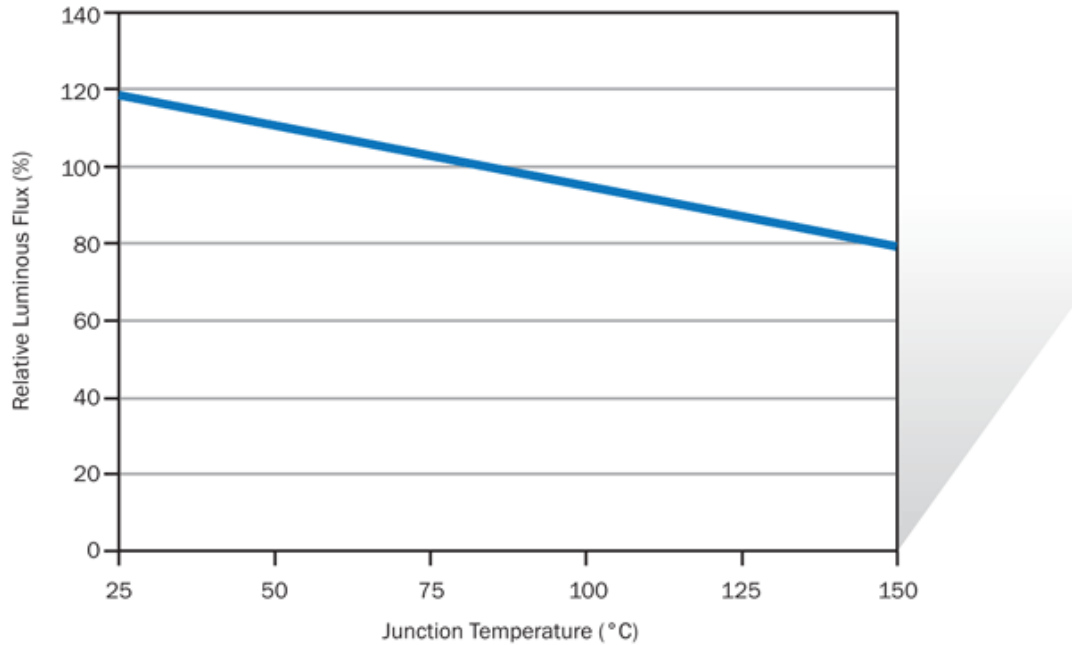


Fig. 1.5 Typical white LED flux vs. junction temperature (Source: Vektrex)

According to basic principles of heat transfer, there are three methods to effectively remove heat from the surface of an object: conduction, convection and radiation. Currently, commonly used methods for electronic device cooling are: air natural convection, forced air, cold air, forced and indirect phase transition cooling, and evaporative cooling. Installation of a mechanical fan is a common method to dissipate heat via forced heat convection. However, this method is not suitable for LED lamps and luminaries because of the limited system weight and size. Also, the copper-based heat sink with mounted LED chips/packages is always exposed to an environment of natural convection. These traditional cooling methods have the disadvantages such as low heat radiation efficiency, complex structure, large volume and high cost. Therefore, radiative cooling becomes attractive for LEDs application since no additional space or power

supply is required. It is reported that, for a natural convection finned heat sink, typically around 25 percent of the total heat can be dissipated via radiation.

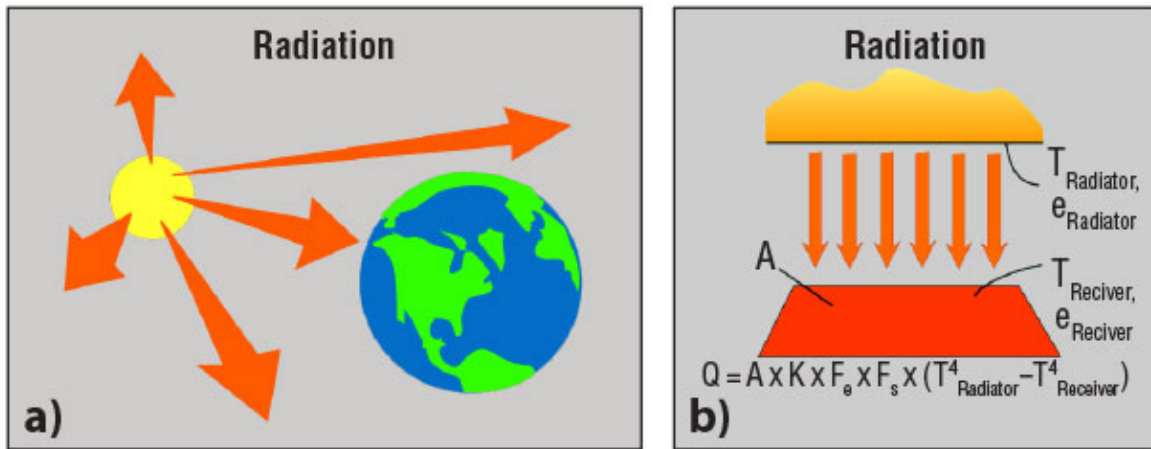


Fig. 1.6. Example of radiation: (a). The sun heating the earth, (b). the radiant heat transfer.

(Source: Dick Bennett, Janus Technologies, private correspondence)

Heat radiation is energy transfer by the emission of electromagnetic waves which carry energy away from the emitting object to its cooler surroundings. In general, all matter emits infrared thermal radiation if the surface temperature is greater than absolute zero. The relationship describing the rate of transfer of radiant energy is called the Stefan-Boltzmann law:

$$P = A\sigma\varepsilon(T^4 - T_c^4)$$

where,  $P$ : net radiation power,  $A$ : surface area,  $T$ : temperature of radiator,  $T_c$ : temperature of surroundings,  $\sigma$ : Stephen-Boltzmann constant,  $5.67 \times 10^{-8} \text{ W/m}^2 \cdot \text{K}^4$ ,  $\varepsilon$ : surface emissivity.

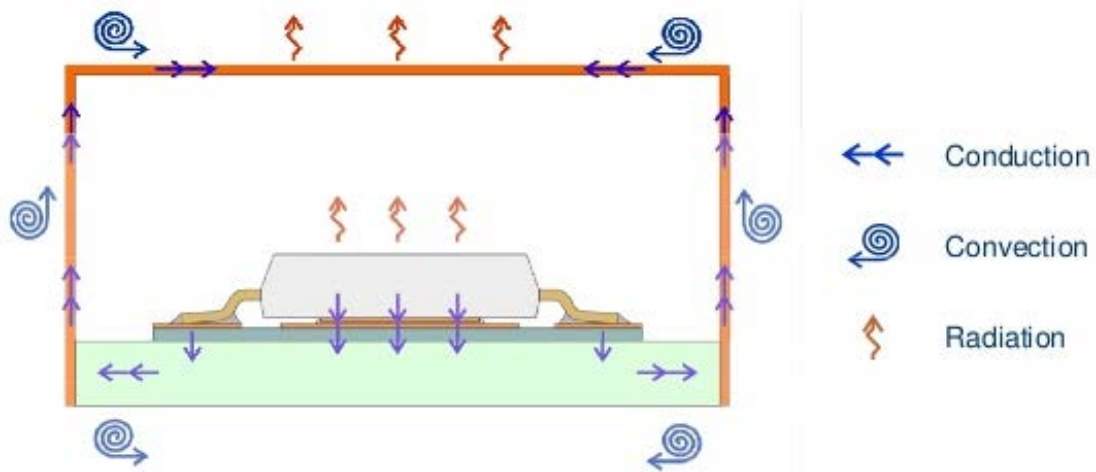


Fig. 1.7. Heat transfer in a LED thermal system. Heat transfer from die to the surrounding environment by conduction, convection and radiation.

(Source: OSRAM)



Recently, the pigmented cooling coatings with high emissivity have been reported to increase the thermal control of electronic systems, cars and buildings. Many researchers study thermal cooling coatings only focusing on the reflectivity and emissivity of coatings in infrared region [11-12]. The cooling coatings proposed in those studies can effectively reduce the surface temperature of objects if the heat source is solar radiation. However, their effectiveness in cooling the electronic devices whose heat source is electric heating, is very questionable. There is still a strong need for the development of radiation cooling coatings for applications in higher power LEDs and LCD backlight units.

## References

1. Gutierrez-Escolar, A. Castillo-Martinez, J. M. Gomez-Pulido, J. M. Gutierrez-Martinez, Z. Stacic, J. A. Medina-Merodio, A Study to Improve the Quality of Street Lighting in Spain. *Energies* 8, 976–994 (2015)
2. J. H. Han, Y. C. Lim, Design of an LLC Resonant Converter for Driving Multiple LED Lights Using Current Balancing of Capacitor and Transformer. *Energies* 8, 2125–2144 (2015)
3. C. J. Weng Advanced thermal enhancement and management of LED packages. *Int. Commun. Heat Mass Transf.* 36, 245–248 (2009)
4. B. Kim, J. Kim, W. Ohm, and S. Kang, “Eliminating hotspots in a multi-chip LED array direct backlight system with optimal patterned reflectors for uniform illuminance and minimal system thickness” *Opt. Express* **18**(8), 8595–A8603 (2010)
5. A. B. Starry, “Diffuse reflective article” US 7,660,040 B2 (2010)
6. C. J. Kaminsky, R. P. Bourdelais, “Light reflector with variable diffuse light reflection” US 0214718 A1 (2003)
7. Y. Taguchi, K. Tomiyoshi, "White thermosetting silicone resin composition for molding an optical semiconductor case and optical semiconductor case." US8013057 B2 (2011)
8. Y. Taguchi, and J. Sawada, “White heat-curable silicone resin composition and optoelectronic part case.” U.S. Patent 8173053 B2, 2013
9. J. Mozzochette, and E. Amaya, “Light emitting diode arrays with improved light extraction.” U.S. Patent 0225222 A1, 2005

10. B. L. Ahn, J. W. Park, S. Yoo, J. Kim, S.B. Leigh and C. Y. Jang, "Saving in cooling energy with a thermal management system for LED lighting in office buildings" *Energies* vol. 8, 6658-6671 (2015)
11. A. P. Raman, M. A. Anoma, L. Zhu, E. Rephaeli, and S. Fan, "Passive radiative cooling below ambient air temperature under direct sunlight." *Nature*, **515**(27) 540-544 (2014)
12. J. A. Johnson, J. J. Heidenreich, R. A. Mantz, P. M. Baker, and M. S. Donley, "A multiple-scattering model analysis of zinc oxide pigment for spacecraft thermal control coatings" *Prog. Org. Coat.*, **47**(3) 432-442 (2003)

## **CHAPTER 2:**

# **STUDY OF OPTIMAL FILLER SIZE FOR HIGH PERFORMANCE POLYMER-FILLER COMPOSITE OPTICAL REFLECTORS**

### **2.1. Introduction**

To reach high conversion efficiencies in optical and photonic devices, advanced light diffusion, distribution and guiding mechanisms need to be employed. High performance optical reflectors are key components for many advanced photonic and optical modules such as those for light emitting diode lighting, LCD display backlighting and photovoltaics [1-3]. High quality diffuse reflectors are also critically important for integrating cavities for accurate quantitative characterization of reflectance and absorption of materials [4-6]. In addition, they are also widely employed for illuminated advertising displays, light boxes for inspection purposes, LED emergency signs, traffic signs and vehicle operators. There is an increasing interest in the development of cost-effective and high performance broadband reflectors in order to decrease the price-performance ratio for optical and photonic devices.

Common optical reflectors employed in optoelectronic application are metallic mirrors, conventional dielectric mirrors and diffusive dielectric composites [7]. Metallic mirrors such as silver and aluminum have high reflectance in the visible light range, but also have the serious drawback of poor long-term stability [8-9]. Conventional dielectric mirrors such as distributed Bragg reflectors (DBR) cannot provide a random light reflecting due to their well-defined geometries. The limited reflection bandwidth of DBR is another issue for its applicability for

solar cells [10]. All-dielectric omnidirectional mirrors can totally reflect electromagnetic waves at all angles with nearly free of loss at optical frequencies, however, their multilayer structures lead to a high production complexity. Diffusive dielectric composites such as polymer-filler reflectors have been demonstrated to be effective reflectors in LED and solar cell technology [11]. These reflectors are embedded with fillers of refractive indices that differing from those of polymeric matrices. In general, polymer-based diffuse reflectors have the advantages of high reflectance over a broad spectral range, low cost, ease of fabrication and high throughput. Recently, silicone-based composites have been used to make high performance reflectors because of their good UV, thermal and environmental stability. Thus, there is a strong need for the development of silicone-based reflecting materials which are more cost-effective and reliable for applications in higher power devices and short wavelength radiation.

Efforts have been made to develop highly reflective polymeric materials for many years because relatively small improvements in the percent reflectivity can have a substantial effect on the amount of energy needed to produce the required lighting [12]. There are many benefits to the optimization of polymer-based reflectors by controlling filler size. With the critical filler size, a reflector can obtain the theoretical maximum reflectance with the lowest filler volume fraction and reflector thickness. Different modeling approaches have already been used to investigate diffuse dielectric reflectors. Monte Carlo simulation is a numerical method with high accuracy but is very costly and time-consuming [13]. The exact radiation transfer theory based on radiation transfer equations (RTE) provides an analytical model, but this model requires heavy calculations and is very difficult to solve without approximations. N-flux one-dimensional models such as Kebulka-Munk model are approximated analytical method providing explicit formulas that are easily utilizable [14]. For industrial application, a simple analytical model is

preferred due to its high computationally efficiency and its ability to provide a deeper understanding of physics behind the high reflectance of polymer-filler composites. There are numbers of reports modeling the scattering efficiency of specific fillers such as TiO<sub>2</sub> and ZnO [16-18]. However, based on our best knowledge, there is no report using a simple analytical model to directly predict the critical size of inorganic fillers with low absorption at short wavelength for diffuse polymer-based reflectors.

In this study, we used a simple analytical model to identify the critical filler size to obtain the highest reflectance while also reducing the filler volume fraction and reflector thickness required. The model prediction was then validated with experimental data. Our results demonstrate for the first time that for different inorganic fillers, a critical filler size ranging from submicron to several microns provide the maximum reflectance for polymeric-filler reflectors. The present results have important implications to the targeted formulation for reflective packaging materials.

## **2.2. Model and prediction**

A simplified schematic diagram of radiation interaction in silicone-filler reflectors is shown in Fig. 1. We assume that the polymer-based diffuse reflector is treated as homogeneous spherical particles of certain radius within the non-absorbing matrix. The fillers used in this experiment are strong scattering and non-absorbing in the wavelength of visible light. Due to the sample preparation method, the specular reflection is negligible and the samples have a largely diffuse appearance.

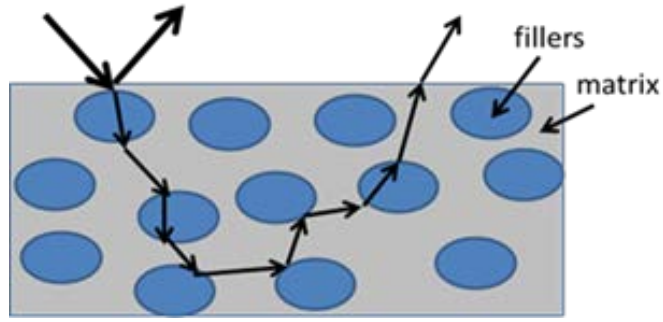


Fig. 2.1. Schematic of light scattering in silicone-filler composite reflectors

In this study, we use the Kubelka-Munk model of reflectance for analysis of diffuse reflectance for weakly absorbing composites [16]. The model works quite well for optically thick materials with high light reflectivity and low transparency if the material is of a constant finite thickness when illumination is diffuse and homogenous, and when no reflection occurs at the surface of materials. The general equation of Kubelka-Munk theory is given:

$$Sx = \frac{1}{\left(\frac{1}{R_\infty} - R_\infty\right)} \ln \left( \frac{1 - RR_\infty}{1 - \frac{R}{R_\infty}} \right) \quad (1)$$

Where  $x$  is the thickness of sample,  $R$  is the reflectance of sample and  $R_\infty$  is the reflectivity of sample materials at infinite thickness. The scattering coefficient per unit thickness ( $S$ ) is a heuristic parameter and can be defined as an expression of scattering efficiency [19]. The scattering behavior of incident light on particles depends on the size parameter ( $X$ ), which is defined as  $X = \pi d/\lambda$ . In the present model, the scattering efficiency was calculated from anomalous diffraction theory (ADT) for particles with large size parameters ( $X \geq 1$ ), and Rayleigh approximation for small size parameters ( $X < 1$ ). ADT is a very approximate but computationally fast technique to calculate extinction, scattering, and absorption efficiencies for many typical size distributions. For large particles, we calculated the extinction efficiency by:

$$Q_{ext} = 2 - \frac{2\lambda}{(n-1)\pi d} \sin\left[\frac{2(n-1)\pi d}{\lambda}\right] + \frac{4\lambda^2}{[2(n-1)\pi d]^2} \left\{1 - \cos\left[\frac{2(n-1)\pi d}{\lambda}\right]\right\} \quad (2)$$

For small particles in the Rayleigh regime, the scattering efficiency for a single particle is given by:

$$Q_{sca} = \frac{8\pi^4}{3} \left(\frac{d^4}{\lambda^4}\right) \left(\frac{n^2-1}{n^2+2}\right) (n_m)^4 \quad (3)$$

Where  $Q_{sca}$  is the scattering efficiency, which is defined as the ratio of the scattering cross section and geometrical cross section  $\pi r^2$ ,  $\lambda$  is the light wavelength,  $d$  is the diameter of spherical particle,  $n$  is the ratio of refractive indices of fillers and matrices, and  $n_m$  is the refractive index of matrix. Based on our assumption, the extinction efficiency ( $Q_{ext}$ ) here is equal to the scattering efficiency considering there is no absorption. For spherical particles, the scattering coefficient ( $S$ ) is usually evaluated as the particle volume fraction times the volumetric scattering cross section of the particle. Here we take into consideration the effects of interfaces between fillers and matrix material and accordingly modified the expression of scattering coefficient as follows:

$$S = \frac{3f}{4V_p} C_{sca} (1-g)Y = \frac{9f}{8d} Q_{sca} (1-g)Y \quad (4)$$

Where  $f$  is the volume fraction of particles in composites,  $C_{sca}$  is the scattering cross section of spheres as a function of diameter  $d$ ,  $V_p$  is the volume of a single particle, and  $g$  is the asymmetry parameter which can be calculated with Mie theory [16].  $Y$  is the correction factor determined by experimental measurements and is constant for  $Al_2O_3$ -silicone composites and  $TiO_2$ -silicone composites.

By entering Eqs. (2) – (4) into Kubelka-Munk general Eq. (1), a simple model for analyzing the reflectance of polymer-based diffuse reflectors is developed. For large filler particles, the formula is:



$$R = \frac{1 - e^{\left\{ \frac{9f}{8d} \left[ 2 - \frac{2\lambda}{(n-1)\pi d} \sin^2 \frac{2(n-1)\pi d}{\lambda} + \frac{4\lambda^2}{[2(n-1)\pi d]^2} \left[ 1 - \cos \frac{2(n-1)\pi d}{\lambda} \right] \right\} x \left( \frac{1}{R_\infty} - R_\infty \right) \right) (1-g)^Y}{R_\infty - e^{\left\{ \frac{9f}{8d} \left[ 2 - \frac{2\lambda}{(n-1)\pi d} \sin^2 \frac{2(n-1)\pi d}{\lambda} + \frac{4\lambda^2}{[2(n-1)\pi d]^2} \left[ 1 - \cos \frac{2(n-1)\pi d}{\lambda} \right] \right\} x \left( \frac{1}{R_\infty} - R_\infty \right) \right) (1-g)^Y} \quad (5)$$

And for small filler particles, the formula is:

$$R = \frac{1 - e^{\left\{ \frac{9f}{8d} \left[ \frac{8\pi^3}{3} \left( \frac{d^4}{\lambda^4} \right) \left( \frac{n^2-1}{n^2+2} \right) (n_m)^4 \right] x \left( \frac{1}{R_\infty} - R_\infty \right) \right\} (1-g)^Y}{R_\infty - e^{\left\{ \frac{9f}{8d} \left[ \frac{8\pi^3}{3} \left( \frac{d^4}{\lambda^4} \right) \left( \frac{n^2-1}{n^2+2} \right) (n_m)^4 \right] x \left( \frac{1}{R_\infty} - R_\infty \right) \right\} (1-g)^Y} \quad (6)$$

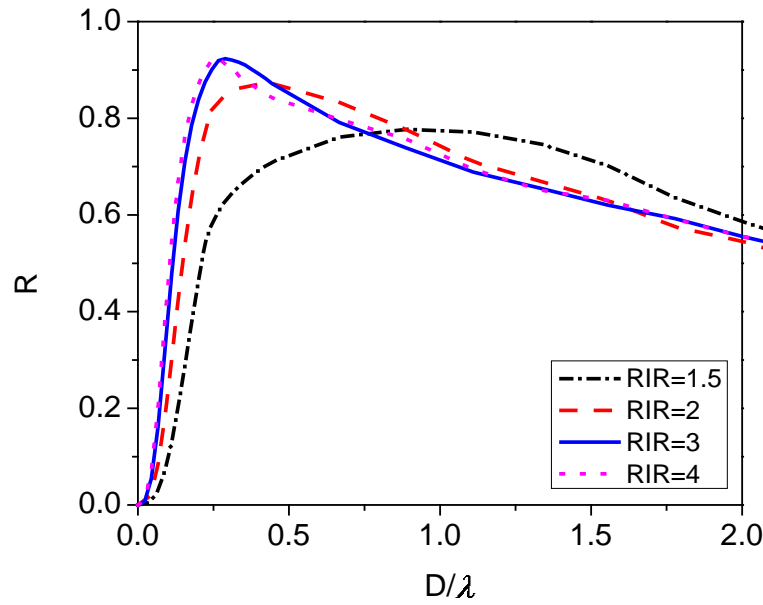


Fig. 2.2. The prediction of reflectance as a function of filler size-wavelength ratio for composite reflectors with different filler-matrix refractive index ratio ( $RIR = n_{\text{filler}}/n_{\text{matrix}}$ ) at wavelength of 450nm.

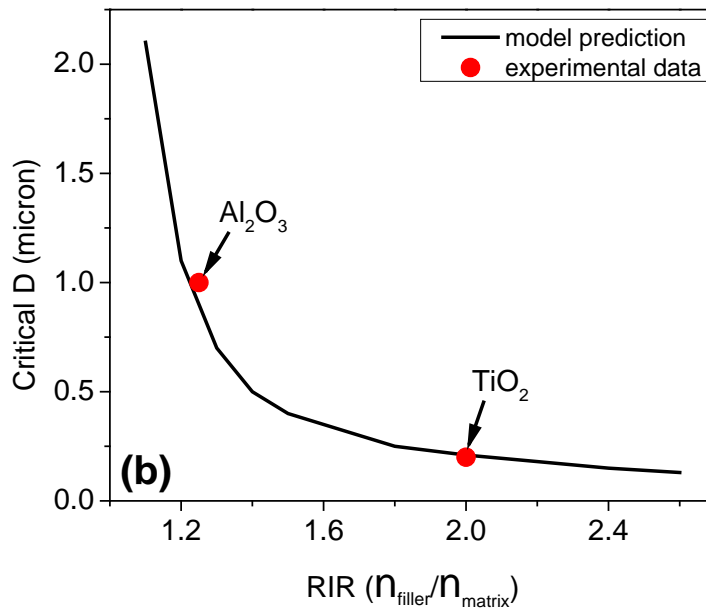
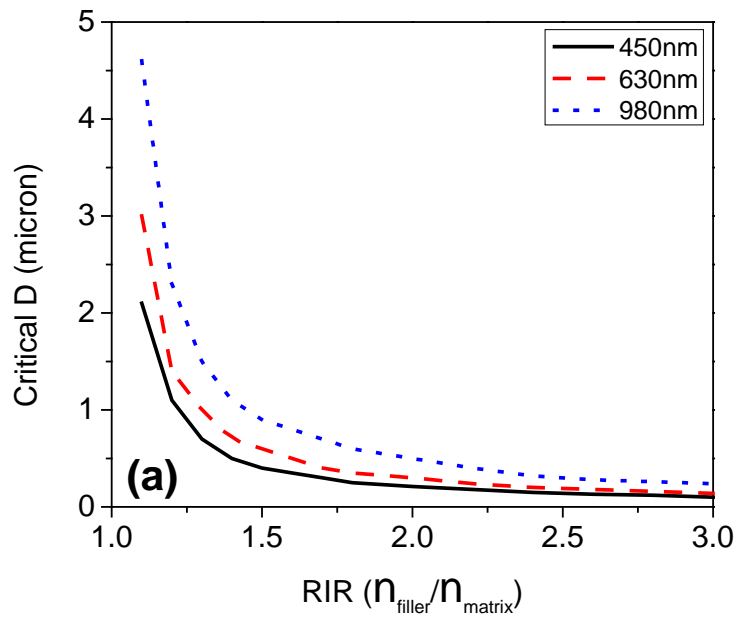


Fig. 2.3. The prediction of critical filler size as a function of RIR (a). for polymer-based reflectors at different wavelength and (b). for silicone-based reflectors at wavelength of 450nm. The symbols indicate the measured optimized filler size with different fillers (left:  $\text{Al}_2\text{O}_3$ , right:  $\text{TiO}_2$ ) and the line shows the calculated optimized filler size based on model.

The main advantage for this new model is that it provides explicit formulas that are easily utilizable to make a number of predictions. The key factors affecting reflectance are filler size, volume fraction, difference between refractive indices between fillers and matrices, and the thickness of reflector [20]. The model predicts critical filler size for different inorganic fillers as shown in Figs. 2 and 3. RIR in Fig. 3 is the filler-matrix refractive index ratio ( $RIR = n_{\text{filler}}/n_{\text{matrix}}$ ). Theoretically, a critical filler size for maximum reflectance exists and needs to be investigated in order to reduce the overall costs of reflectors.

## **2.3. Experimental results and discussion**

### 2.3.1 Experimental

In order to identify the critical filler size for composite reflectors required to obtain the highest reflectance, as well as to compare experimental data versus the modeling prediction, silicone based composites were prepared using inorganic fillers with various particle size at a volume fraction of 0.1. The inorganic fillers used in this experiment are  $\text{Al}_2\text{O}_3$  (from Inframat Advanced Materials Inc) and  $\text{TiO}_2$ . The diameters of  $\text{Al}_2\text{O}_3$  particles were 0.04, 0.08, 0.1, 0.3, 1, 10, 20 and 35 micron. The diameters of  $\text{TiO}_2$  particles were 0.04, 0.1, 0.2, 0.5 and 5 micron. The refractive indices at a wavelength of 450nm are 1.78 for  $\alpha\text{-Al}_2\text{O}_3$  particles and 2.81 for rutile- $\text{TiO}_2$  particles. The matrix material was a high performance silicone formulated by Shi's lab [21]. The silicone has a refractive index of 1.40 at a wavelength of 450nm and is high in transparency.

The silicone composites were fabricated by mixing silicone resin with various amounts of inorganic fillers using a Thinky high shear mixer at 2500 r/min for 5 minutes. After mixing, the composites were degassed under a vacuum of 10-2 Pa for 30 minutes in order to get rid of the

trapped air bubbles introduced during the mixing. The mixture was then transferred into a stainless steel mold and followed by a curing at 150°C for 2.5 hours to solidify the composites. The prepared composites had a plate shape with a diameter of 22mm.

The fabricated composite was repeatedly polished using a South Bay Technology polisher. The light reflectance of the composites, at a wavelength range from 400 to 1000 nm, was measured using a conventional light reflectometer (Filmetrics, Model F20) with an integral sphere.



Fig. 2.4. The Thinky centrifuge mixer for silicone matrix and filler mixing



Fig. 2.5. The vacuum oven for degassing (Fisher scientific, Model 280A)

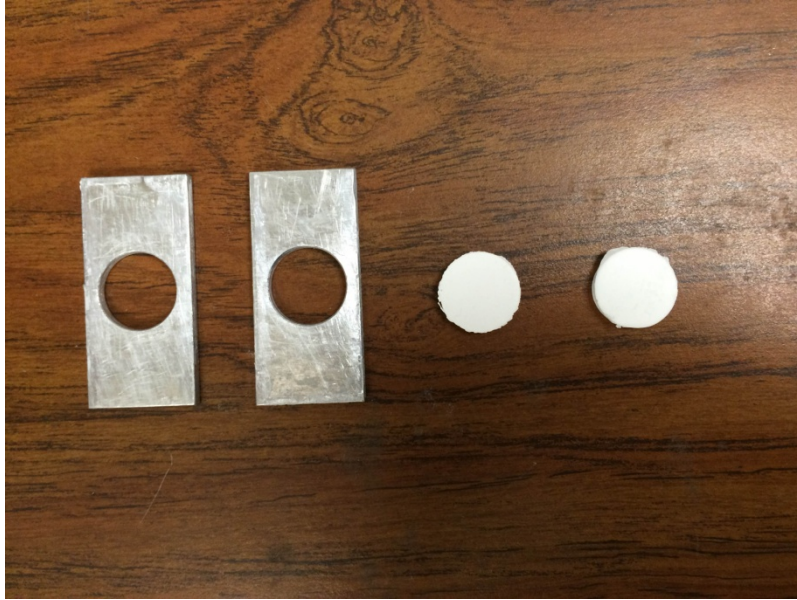


Fig. 2.6. The stainless steel molds and molded reflector samples

### 2.3.2 Verification of model and optimization of reflectors

The reflectance properties of two types of inorganic fillers were calculated using ADT and Rayleigh scattering approximation coupled with Kubelka-Munk model. To validate the accuracy of model prediction, we compared our calculation results to the experimental measurements. Figure 2.7 shows the comparison between the model's predictions and experimental data for reflectance of silicone-based reflectors as a function of filler size at a wavelength of 450nm. For better comparison, reflectance is normalized by setting the highest value as 1. The highest value of raw reflectance is 93% for  $\text{Al}_2\text{O}_3$ -silicone composites and 94% for  $\text{TiO}_2$ -silicone composites.

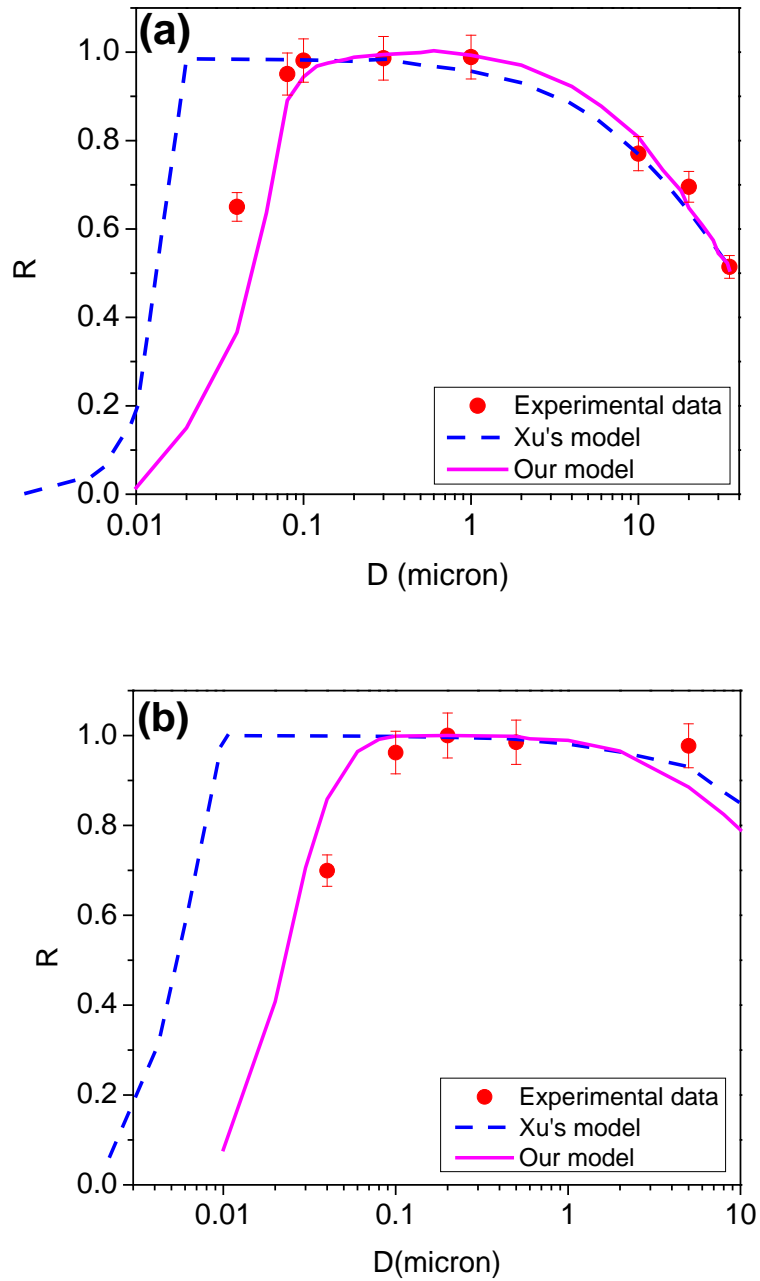


Fig. 2.7. Normalized reflectance vs. particle size for 3mm thick (a)  $\text{Al}_2\text{O}_3$ -silicone composites and (b)  $\text{TiO}_2$ -silicone composites at wavelength of 450nm with 0.1 filler volume fraction. For better comparison, reflectance is normalized by setting the highest value as 1. The circles indicate the measured reflectance and the lines show the calculated reflectance based on model.



Also shown is the prediction based on the simple analytical model for coating system developed by Wenlan Xu. Xu's model abandons Mie theory and reverts to a combination of geometrical optics and wave optics to calculate the main scattering and absorption coefficients. The details of this model are given by W. Xu and S.C. Shen [22], and Emslie and Aronson [23]. From the plots in Fig. 2.7, it is evident that our model better fits the existing experimental data than Xu's model. Xu's model is able to predict the reflectance for composites with filler sizes similar to and larger than light wavelength. However, it cannot achieve a good fit for fillers at a size smaller than this wavelength and therefore, its applicability for determining the critical filler size of polymer-based reflectors with small size parameters is still questionable.

Figure 2.7 also indicates that the effect of filler size on light reflectance is non-monotonic. For these two fillers, the light reflectance increases as the particle size increases from nano-size to submicron-size, and then decreases as the particle size increases to micron sizes. The critical size for fillers to effectively reflect incident radiation at a 450nm wavelength is 0.8 microns for  $\text{Al}_2\text{O}_3$  pigment, and 0.2 microns for  $\text{TiO}_2$  pigment. The predicted critical filler size of  $\text{TiO}_2$  particles shows a good agreement with Vargas's results [12]. In the case of nano-size particles, the effect of refractive index mismatch on light scattering is usually less important than the effect of particle size. A high amount of visible light is transmitted by composites with nano-size particles. The reason for the maximum reflectance of composites with submicron-size fillers is because of its high light scattering coefficient. It is also known from Mie theory that when the size of particle is comparable to the wavelength of incident light, the magnitude of scattering efficiency reaches its maximum. This light reflectance decrease with increasing particle size due to the decrease in effective scattering cross sections. The total surface area for larger particles is lower because at the same volume fraction, the number of smaller particles is much more than

that of larger particles. It is demonstrated those modeling results give us a good indication of what particle sizes of fillers are most effective than others for specific fillers at a particular wavelength.

The theoretical critical filler size as a function of the refractive index ratio between filler and matrix for different inorganic fillers at a wavelength of 450nm is shown in Fig. 3b. Overall, there is a good agreement between calculation results and experimental data for samples with different fillers. The results show that the optimized filler size is negatively related to refractive index ratio. The model calculations show that for filler-to-matrix ratios from 1.1 to 2.6, the best reflectance is achieved when the filler sizes used in the reflector are between submicron and several microns. The results provide an important insight for the selection of filler sizes for producing high reflective polymer-based reflectors. In this experiment, we used a silicone matrix and mixed it with different inorganic fillers to produce reflectors. In fact, the same effect shown in the plot can be alternatively made by using other polymer matrices with different refractive indices. Thus, this model can be employed to optimize not only silicone-based reflectors, but also all other polymer-based reflectors in order to increase their reflectance.

Generally, high filler volume fractions and reflector thicknesses are desired for obtaining high reflectance in polymer-based reflectors. However, there is a critical value of filler sizes that enables all inorganic fillers to achieve high reflectance without increasing filler volume fraction and film thickness. The improvements in reflectivity for polymer-based reflectors can be realized by using optimized filler particles. Our results demonstrate for the first time that for different inorganic fillers, a critical filler size ranging from submicron to several microns provides the maximum reflectance. We have demonstrated that our simple analytical model provides a very effective method for optimizing the polymer-based reflectors in LED and solar cell applications.

Furthermore, the accuracy loss of the present model is not very significant for the polymer-based diffuse reflectors studied in the paper.

## **2.4. Conclusion**

In this study, we utilized modeling techniques to investigate the critical sizes of inorganic fillers required to obtain the highest reflectance. The key model predictions were verified by comparisons with experimental data. The light reflectance of tested reflectors increased as the particle size increased from nano-size to submicron-size, and then decreased as the particle size continues to increase to micron-size. The critical size for fillers to effectively reflect incident radiation at 450nm wavelength is around 0.8 microns for  $\text{Al}_2\text{O}_3$  pigments, and 0.2 microns for  $\text{TiO}_2$  pigments. Our results demonstrate for the first time that for different inorganic fillers, a critical filler size that ranges from one submicron to several microns provides the maximum reflectance for polymer-based reflectors. The results provide an empirical basis for selecting filler sizes to produce cost-effective polymer-based diffuse reflectors, while also reducing overall weight.

## References

1. Y. Taguchi, and J. Sawada, "White heat-curable silicone resin composition and optoelectronic part case." US Patent No. 8,173,053 B2 (2012)
2. J. Mozzochette, and E. Amaya, "Light emitting diode arrays with improved light extraction." US Patent No. 0225222 A1 (2005)
3. E. Moulin, U.W. Paetzold, H. Siekmann, J. Worbs, A. Bauer, and R. Carius, "Study of thin-film silicon solar cell back reflectors and potential of detached reflectors." *Energy Procedia* **10**, 106-110 (2011)
4. J. N. Bixler, M. T. Cone, B. H. Hokr, J. D. Mason, E. Figueroa, E. S. Fry, V. V. Yakovlev, and M. O. Scully, "Ultrasensitive detection of waste products in water using fluorescence emission cavity-enhanced spectroscopy" *Proc. Natl. Acad. Sci. U. S. A* **111**(20), 7208-7211 (2014)
5. R. M. Pope, and E. S. Fry, "Absorption spectrum (370-700nm) of pure water. II. Integrating cavity measurements" *Appl. Opt.* **36**(33), 8710-8723 (1997)
6. S. A. Prahl, M. J. C. van Gemert, and A. J. Welch, "Determining the optical properties of turbid media by using the adding-doubling method" *Appl. Opt.* **32**(4), 559-568 (1993)
7. A. Lin, S. M. Fu, Y. K. Zhong, C. W. Tseng, P. Y. Chen, and N. P. Ju, "The rigorous wave optics design of diffuse medium reflectors for photovoltaics" *J. Appl. Phys.* **155**, 153105 (2014)
8. M. Kumei, T. Sakai, and M. Sato, "Light emitting device with a porous alumina reflector made of aggregation of alumina particles" US Patent No. 8,106,413 B2 (2012)
9. H. Gao, H. Chen, X. Zhang, P. Zhang, J. Liu, H. Liu and Y. Cui, "High-performance GaN-based light-emitting diodes on patterned sapphire substrate with a novel hybrid Ag mirror

- and atomic layer deposition-TiO<sub>2</sub>/Al<sub>2</sub>O<sub>3</sub> distributed Bragg reflector backside reflector” *Opt. Eng.* **52**(6), 063402 (2013)
10. A. Lin, Y. K. Zhong, S. M. Fu, C. W. Tseng, and S. L. Yan, “Aperiodic and randomized dielectric mirrors: alternatives to metallic back reflectors for solar cells” *Opt. Express* **22**(S3), A880-A894 (2014)
  11. O. Berger, D. Inns, and A. G. Aberle, “Commercial white paint as back surface reflector for thin-film solar cells” *Sol. Energy Mater. Sol. Cells* **91**(13), 1215-1221 (2007)
  12. D. Chundury, R. Abrams, R.M. Harris, M. Ali, T.G. McGee, and S.T. Schmidt, “Light reflecting polymeric compositions” U.S. Patent 6,838,494 B2, (2002)
  13. B. Maheu, J. N. Letoulouzan, and G. Gouesbet, “Four-flux models to solve the scattering transfer equation in terms of Lorenz-Mie parameters” *Appl. Opt.* **23**(19), 3353-3362 (1984)
  14. W. E. Vargas, and G. A. Niklasson, “Applicability conditions of the Kubelka-Munk theory” *Appl. Opt.* **36**(22), 5580-5586 (1997)
  15. W. E. Vargas, “Optimization of the diffuse reflectance of pigmented coatings taking into account multiple scattering” *J. Appl. Phys.* **88**(7), 4079-4084 (2000)
  16. J. C. Auger, R. G. Barrera, and B. Stout, “Scattering efficiency of clusters composed by aggregated spheres” *J. Quant. Spectrosc. Radiat. Transf.* **79-80**, 521-531 (2003)
  17. J. A. Johnson, J. J. Heidenreich, R. A. Mantz, P. M. Baker, and M. S. Donley, "A multiple-scattering model analysis of zinc oxide pigment for spacecraft thermal control coatings" *Prog. Org. Coat.* **47**(3), 432-442 (2003)
  18. W. E. Vargas, A. Amador and G. A. Niklasson, "Diffuse reflectance of TiO<sub>2</sub> pigmented paints: Spectral dependence of the average pathlength parameter and the forward scattering ratio" *Opt. Commun.* **261**(1), 71-78 (2006)

19. J. E. Moersch, and P. R. Christensen, "Thermal emission from particulate surfaces: A comparison of scattering models with measured spectra" *J. Geophys. Res.* **100**(E4), 7465-7477 (1995)
  20. N. T. Tran, J. P. You and F. G. Shi, "Effect of phosphor particle size on luminous efficacy of phosphor-converted white LED" *J. Lightwave Technol.* **27**(22), 5145-5150 (2009)
  21. L. Y. Her, J. P. You, Y. C. Lin, N. T. Tran, and F. G. Shi, "Development of High-Performance Optical Silicone for the Packaging of High-Power LEDs" *IEEE Trans. Compon. Packag. Technol.* **33**(4), 761-766 (2010)
  22. W. Xu, and S. C. Shen, "Infrared radiation and reflection in an inhomogeneous coating layer on a substrate" *Appl. Opt.* **31**(22), 4486-4496 (1992)
- A. E. Emslie, and J. R. Aronson, "Spectral reflectance and emittance of particulate materials. 1: theory" *Appl. Opt.* **12**(11), 2563-2572 (1973)

**CHAPTER 3:**

**EXPLORING THE CRITICAL THICKNESS FOR MAXIMUM  
REFLECTANCE OF OPTICAL REFLECTORS BASED ON POLYMER-  
FILLER COMPOSITES**

**3.1. Introduction**

High performance optical reflectors for LED lighting, backlighting and solar cells are commonly accomplished by metallic as well as multi-layer dielectric mirrors [1-5]. Polymer-filler composite reflectors have gained great attention as a potential alternative, because of easier manufacturing as well as low cost [6]. In addition, since the polymer-filler composites scatter light in a diffuse pattern, they can improve uniformity and brightness of light distribution, eliminate “dots” and glare for better overall optical aesthetics for LED lighting and LCD backlighting applications [3,7-9].

Among many factors, the reflectance is a function of the thickness of polymer-filler composite. A reduction in thickness of reflectors will be beneficial to the design and manufacturing of display systems in various mobile devices [10,11]. Thus, a deep understanding of reflectance dependence on reflector thickness may accelerate the optimization and development of polymer-filler composite reflectors. In this regard, the Kebulka-Munk approximations are widely adopted in modeling the optical reflectance, and so far, none of those modeling investigations suggest a critical thickness at which the optical reflectance of a polymer-filler reflectors reaches its maximum. Therefore, an analytical study of the critical

thickness for maximum reflectance is essential for developing cost effective high performance reflectors with optimized thickness.

In our previous study, we have developed a simple analytical model with high computational efficiency which is accurate in predicting the filler size dependence of thick polymer-filler reflectors [12]. However, the model does not consider any contribution from substrate and thus it is not applicable for thin polymer-filler optical reflectors on substrates. Thus, the objective of the present work is to modify our prior model to include the effect of the substrate. The model predicts the existence of a critical thickness at which the optical reflectance of a polymer-filler composite reaches its maximum value. The dependence of the critical thickness on back reflection of the substrate, filler volume fraction, filler size, as well as the matrix-filler refractive indices difference is investigated. The analytical model developed, which is expected to be valuable for accelerating the design and optimization of polymer-filler composite reflectors is verified experimentally.



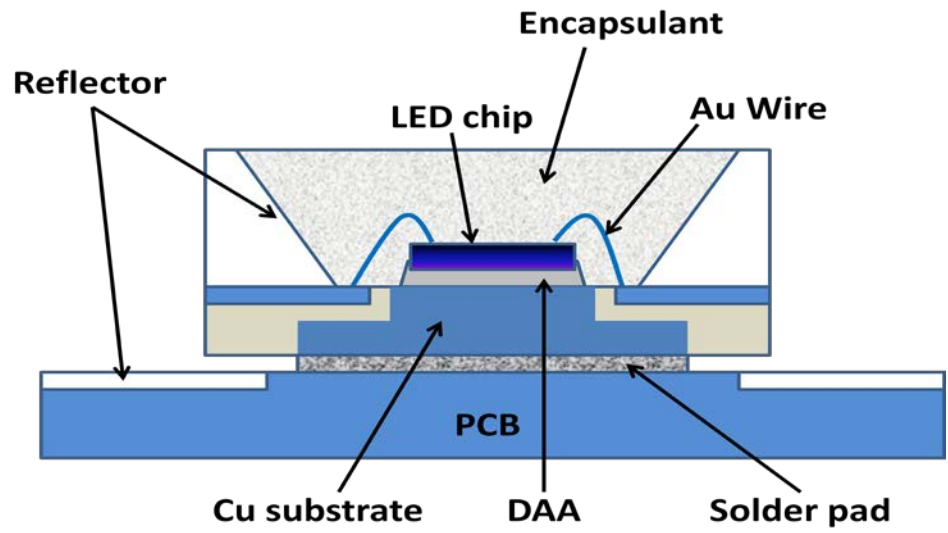


Fig. 3.1. The schematic cross-sectional view of a LED package.

### 3.2. Experiment

In the experiment, polymer-filler composite reflectors were fabricated by mixing transparent silicone resin with inorganic fillers. The inorganic fillers used for the samples are Boron nitride (BN) and Zinc oxide (ZnO) (from Sigma-Aldrich and Inframat Advanced Materials Inc), which are two common inorganic pigments used in coating industry. The properties of materials used in polymer-filler reflectors are listed in Table 3.1.

In order to form a homogenous mixture, various amounts of filler were mixed with high performance silicone using a Shinky high shear mixer at 2500 r/min for 5 minutes. After mixing, the composites were degassed under a vacuum of  $10^{-2}$  Pa for 30 minutes in order to get rid of the trapped air bubbles. The mixture was then coated on to mirror-like Cu or Al substrates using film applicator and cured at 150°C for 2 hours.

The light reflectance of the fabricated reflectors at a wavelength range from 400 to 1000 nm was measured using a conventional light reflectometer (Filmetrics Model F20). The thickness of reflectors was measured using coating thickness gauge (CEM Model DT-156).

Table 3.1. Properties of materials used for samples

Materials	Refractive index ( $\lambda =$ 450 nm)	Average particle size ( $\mu\text{m}$ )
BN powders	1.81 [13]	1
ZnO powders	2.11 [13]	1
Silicone resin	1.42 [14]	-



Fig. 3.2. The BYK thin film applicator for reflective films preparation



Fig. 3.3. The coating thickness gauge for thickness measurement (CEM Model DT-156)

### 3.3. Analysis

#### 3.3.1 Model

The interaction of incident radiance with a single particle is characterized in terms of scattering and absorption cross section,  $C_{sca}$  and  $C_{abs}$  respectively. The sum of scattering and absorption cross section is called extinction cross section ( $C_{ext}$ ). Anomalous Diffraction Theory (ADT) is an approximate but computationally fast method to calculate above-mentioned efficiencies for particles with a size larger or equal to the wavelength of light [15-18]. Rayleigh Scattering Theory is a more accurate method to describe the scattering behavior of particles which are smaller compared to the wavelength of light [19,20]. Based on these two theories,  $C_{ext}$  can be expressed as a function of geometrical cross section ( $\pi r^2$ ), light wavelength ( $\lambda$ ), size of filler particle ( $d$ ), the ratio of refractive indices of fillers and matrices ( $n$ ), and the refractive index of matrix ( $n_m$ ). Since the absorption of fillers is negligible, the scattering efficiency is equal to the extinction efficiency.

The scattering cross section of large particles is calculated based on ADT:

$$C_{sca} = \frac{\pi d^2}{4} \left\{ 2 - \frac{2\lambda}{(n-1)\pi d} \sin \left[ \frac{2(n-1)\pi d}{\lambda} \right] + \frac{4\lambda^2}{[2(n-1)\pi d]^2} \left( 1 - \cos \frac{2(n-1)\pi d}{\lambda} \right) \right\} \quad (1)$$

The scattering cross section for particles in Rayleigh regime is calculated according to Rayleigh scattering theory:

$$C_{sca} = \frac{2\pi^5 d^2}{3} \left( \frac{d^4}{\lambda^4} \right) \left( \frac{n^2 - 1}{n^2 + 2} \right) (n_m)^4 \quad (2)$$

In order to better understand and investigate the critical thickness, we developed an analytical model to describe the relationship between reflectance and thickness of reflectors. In this study, the polymer-filler composite reflectors are treated as monosized spherical particles embedded in

the non-absorbing matrix. Both BN and ZnO fillers are strong scattering and non-absorbing in the wavelength of visible light. We assume that all of the samples have a largely diffuse appearance and the specular reflection is negligible. The Kubelka-Munk model is employed for describing the optical properties of polymer-filler reflectors. In this two-flux model, the incident light is considered to consist of two isotropic diffuse fluxes travelling both upwards ( $I_d$ ) and downwards ( $J_d$ ) through the material. The differential equations for the intensities of two diffuse fluxes are:

$$\frac{dI_d}{dx} = -(S + K)I_d + SJ_d \quad (3)$$

$$\frac{dJ_d}{dx} = (S + K)J_d + SI_d \quad (4)$$

Since most of reflective coatings are painted on substrates in real coatings application, we assume there is radiation leak out through the back side of reflectors and back reflected radiation from the substrate need to be included in the model. The solution of diffuse reflection ( $R$ ) using Kubelka-Muck model is:

$$Sx = \frac{1}{\frac{1}{R_\infty} - R_\infty} \ln \left( \frac{R' - R_\infty}{R' - \frac{1}{R_\infty}} \times \frac{1 - RR_\infty}{1 - \frac{R}{R_\infty}} \right) \quad (5)$$

where  $x$  is the thickness of the reflector, which is measured perpendicular to the illuminated side.  $S$  and  $K$  are scattering and absorption coefficient per unit length, respectively.  $S$  for spheres can be expressed as a function of filler volume fraction ( $f$ ), volumetric scattering cross section ( $C_{sca} / V$ ) and correction factor  $Y$ .  $R'$  is the back reflection from substrates and  $R_\infty$  is the reflectivity of reflector with infinite thickness.

$$S = \frac{3f}{4V_p} C_{sca} (1 - g) Y \quad (6)$$

Finally, we obtained the expression of reflectance for large fillers as:

$$R(x) = \frac{\left( \frac{R' - \frac{1}{R_\infty}}{R' - R_\infty} \right) R_\infty e^{\left\{ \frac{9f}{8d} \left[ 2 - \frac{2\lambda}{(n-1)\pi d} \sin \frac{2(n-1)\pi d}{\lambda} + \frac{4\lambda^2}{[2(n-1)\pi d]^2} [1 - \cos \frac{2(n-1)\pi d}{\lambda}] \right\} x \left( \frac{1}{R_\infty} - R_\infty \right) \right)^{(1-g)Y} - \frac{1}{R_\infty}}{\left( \frac{R' - \frac{1}{R_\infty}}{R' - R_\infty} \right) e^{\left\{ \frac{9f}{8d} \left[ 2 - \frac{2\lambda}{(n-1)\pi d} \sin \frac{2(n-1)\pi d}{\lambda} + \frac{4\lambda^2}{[2(n-1)\pi d]^2} [1 - \cos \frac{2(n-1)\pi d}{\lambda}] \right\} x \left( \frac{1}{R_\infty} - R_\infty \right) \right)^{(1-g)Y} - 1} \quad (7)$$

And the expression for small fillers as:

$$R(x) = \frac{\left( \frac{R' - \frac{1}{R_\infty}}{R' - R_\infty} \right) R_\infty e^{\left\{ \frac{9f}{8d} \left[ \frac{8\pi^3}{3} \left( \frac{d^4}{\lambda^4} \right) \left( \frac{n^2-1}{n^2+2} \right) (n_m)^4 \right\} x \left( \frac{1}{R_\infty} - R_\infty \right) \right)^{(1-g)Y} - \frac{1}{R_\infty}}{\left( \frac{R' - \frac{1}{R_\infty}}{R' - R_\infty} \right) e^{\left\{ \frac{9f}{8d} \left[ \frac{8\pi^3}{3} \left( \frac{d^4}{\lambda^4} \right) \left( \frac{n^2-1}{n^2+2} \right) (n_m)^4 \right\} x \left( \frac{1}{R_\infty} - R_\infty \right) \right)^{(1-g)Y} - 1} \quad (8)$$

In general, the reflectance (R) increases as back reflection (R'), thickness (x), refractive index ratio between matrices (n), reflectivity of reflectors (R<sub>∞</sub>) and filler volume fraction (f) increase. Therefore, it is desired to have high values of all these parameters in order to obtain a high reflectance of polymer-filler reflectors.

### 3.3.2 Model prediction

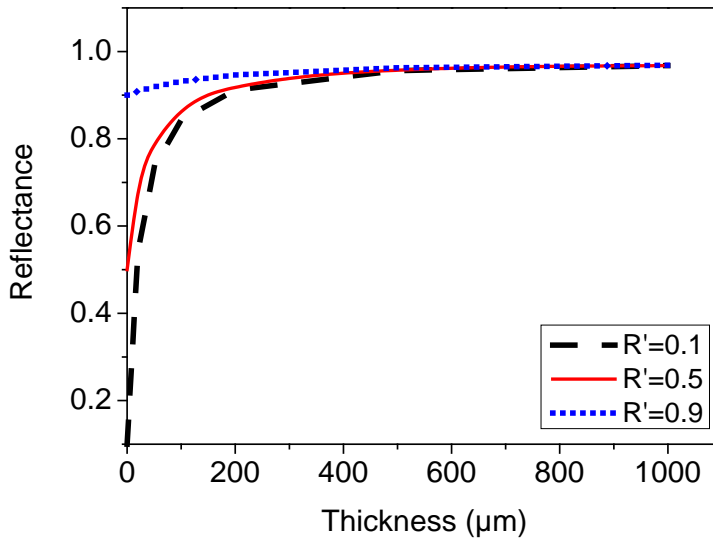


Fig. 3.4. The prediction of reflectance as a function of thickness of reflector for different back reflection from substrate.

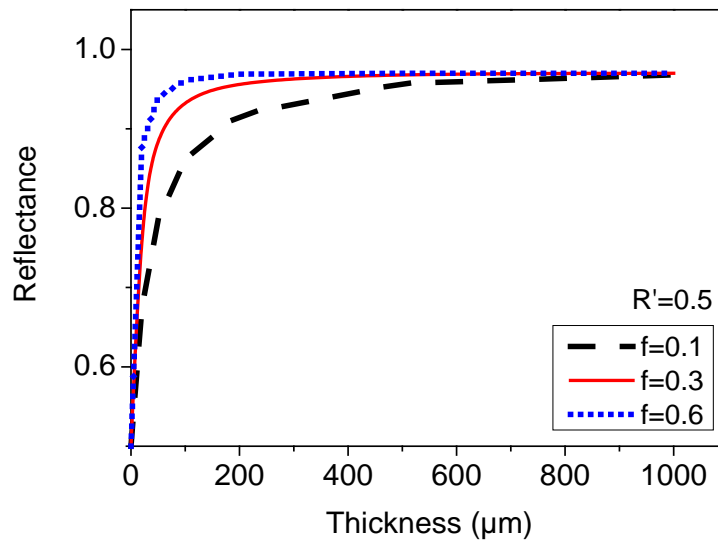


Fig. 3.5. The prediction of reflectance as a function of reflector thickness of reflector for different filler volume fraction.

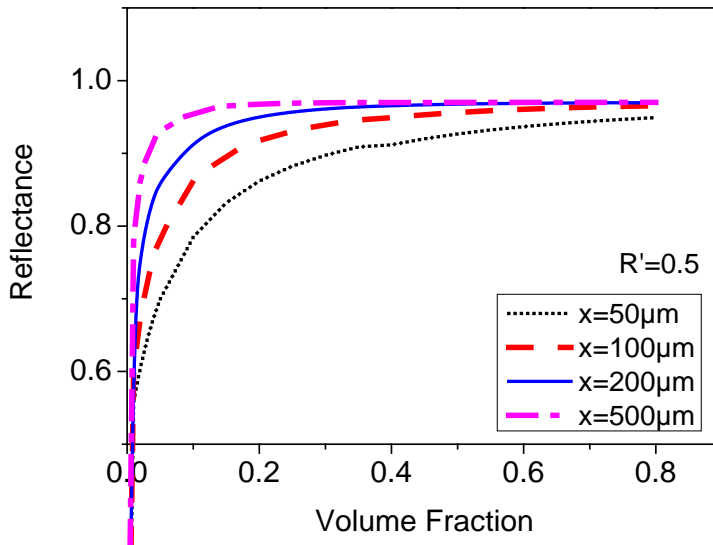


Fig. 3.6. The prediction of reflectance as a function of volume fraction of reflector.

According to equations (7) and (8), the reflectance is strongly dependent on back reflection from substrate, reflector thickness and filler volume fraction. Some key predictions were made and the assumed filler size is  $1\ \mu\text{m}$ , refractive index ratio between filler and matrix is 1.3. The targeted wavelength is  $450\ \text{nm}$ , which is the emission peak of blue LED chips. Our model predicts that the change of reflectance with thickness of reflectors and filler volume fraction as shown in Figs. 4, 5 and 6. Our model also predicts that the critical thickness, where the reflector approach its saturation reflectance, decreases with increasing of the back reflection from substrate and the filler volume fraction, as demonstrated in Figs. 4 and 5. Since the critical thickness is the minimum thickness capable of providing theoretical maximum reflectance, this model can be applied to investigate the critical thickness of reflectors in order to reduce the overall volume and weight of display systems for various mobile devices, such as smart phones, tables and ultrabooks.



### 3.4. Result and discussion

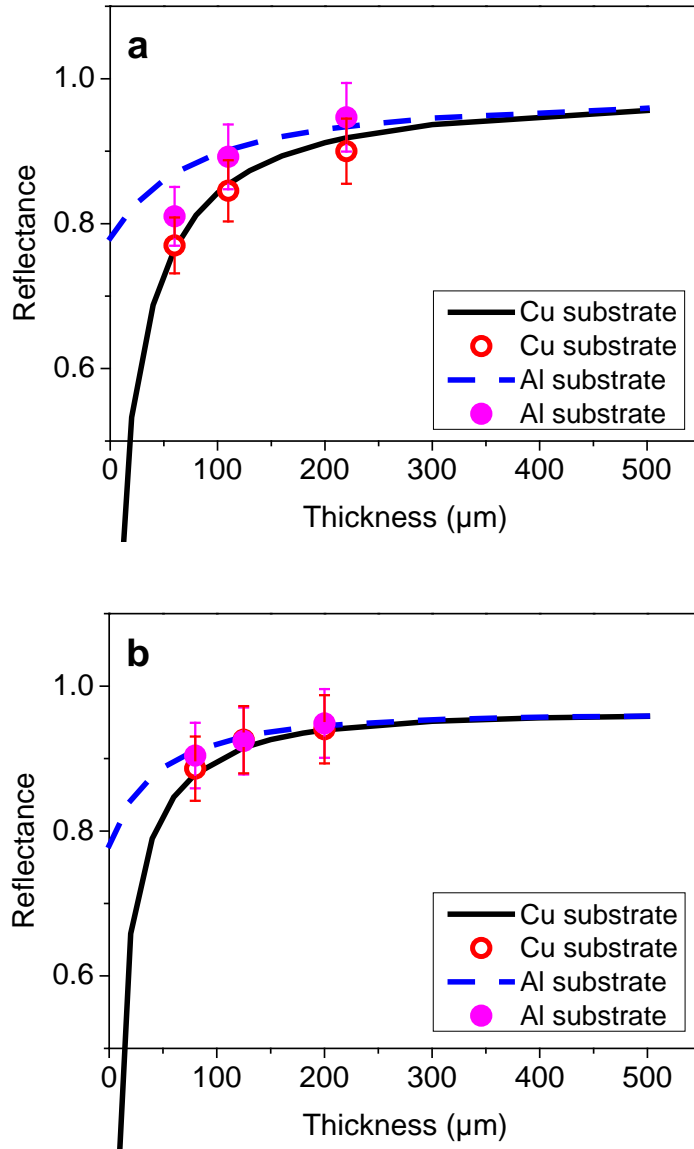


Fig. 3.7. Reflectance change of (a) BN-silicone coatings and (b) ZnO-silicone coatings on Cu substrate ( $R'=0.07$ ) and Al substrate ( $R'=0.78$ ) at wavelength of 450nm. The filler volume fraction is 0.1. The symbols indicate the measured reflectance with different thickness ( $x$ ) and the lines show the theoretical reflectance based on model.

In order to investigate the influence of thickness, thin layers of reflective coatings were painted onto the Cu and Al substrates. The experimental data was measured by a reflectometer and an integrating sphere. The comparisons between calculated results and measured reflectance as a function of thickness for BN-silicone and ZnO-silicone reflectors are presented in Fig. 5.7. All the reflectances are taken at wavelength of 450 nm, which is the emission peak of blue LED chips. There is a good agreement between calculation results and experimental data for samples with different substrates. It is shown that a non-linear relationship between increase in reflectance and thickness of reflector. As can be seen from Fig.3.7 (a), the reflective coating sample on Cu substrate requires a thickness of about 200  $\mu\text{m}$  to reach its saturation reflectance, while for the sample on Al substrate, the corresponding thickness is only about 100  $\mu\text{m}$ . It is concluded that a thinner layer of reflective coating is needed for a substrate with higher reflectance in order to obtain the same effect.

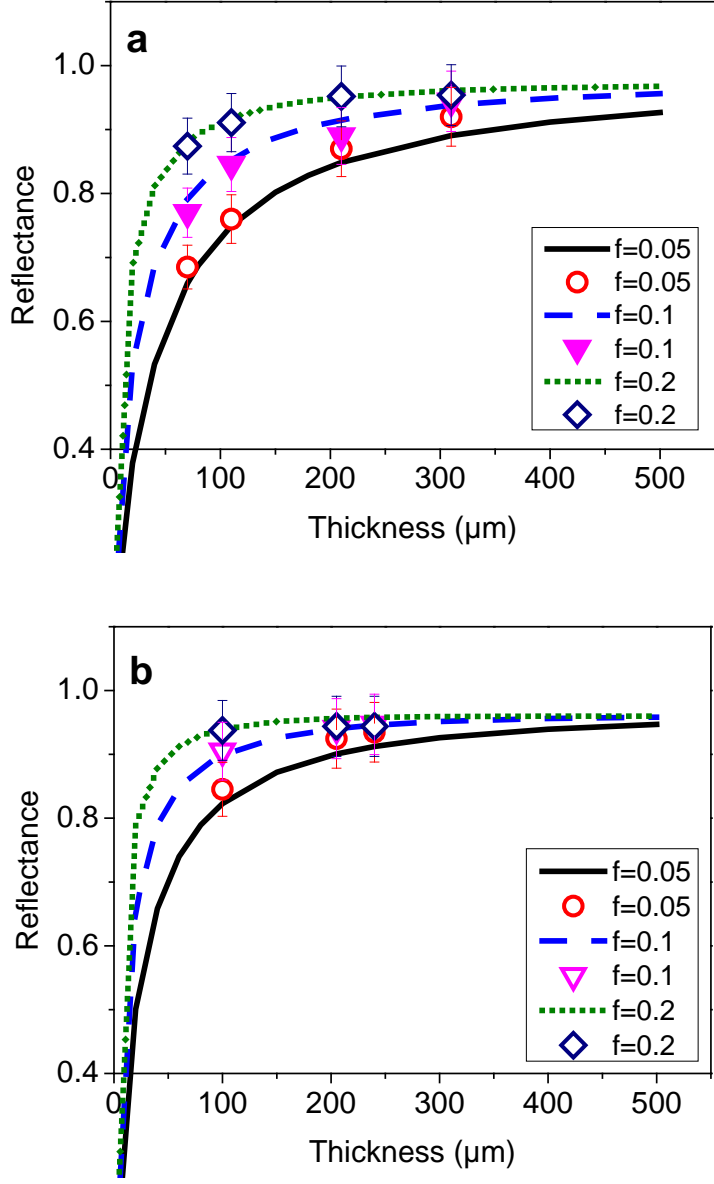


Fig. 3.8. Reflectance vs. reflector thickness for (a) BN-silicone coatings and (b) ZnO-silicone coatings on Cu substrate ( $R'=0.07$ ) at wavelength of 450nm. The symbols indicate the measured reflectance with different filler volume fraction ( $f$ ) and the lines show the theoretical reflectance based on model.

The theoretical and experimental reflectances as a function of reflector thickness for BN-silicone and ZnO-silicone reflectors are shown in Figure 3.8. The theoretical results are found to be consistent with experimental data, verifying the optimization trends calculated by the modeling. For both types of reflectors, the reflectance increases rapidly from very small thickness to a critical thickness, and then reaches stabilization as the reflector gets thicker. The scattering interfaces between fillers and matrix within the composite reflectors increases as total thickness increases, resulting in a boost of reflectance for reflectors with a thickness smaller than the critical value. As the thickness further increases, the absorption of light by silicone matrix causes the saturation of reflectance, and therefore it is unnecessary to make a reflector thicker. For BN-silicone reflectors, the critical thickness at which the reflectance becomes stable is around 200  $\mu\text{m}$ ; for ZnO-silicone reflectors, the critical thickness to provide stable reflectance is around 100  $\mu\text{m}$ .

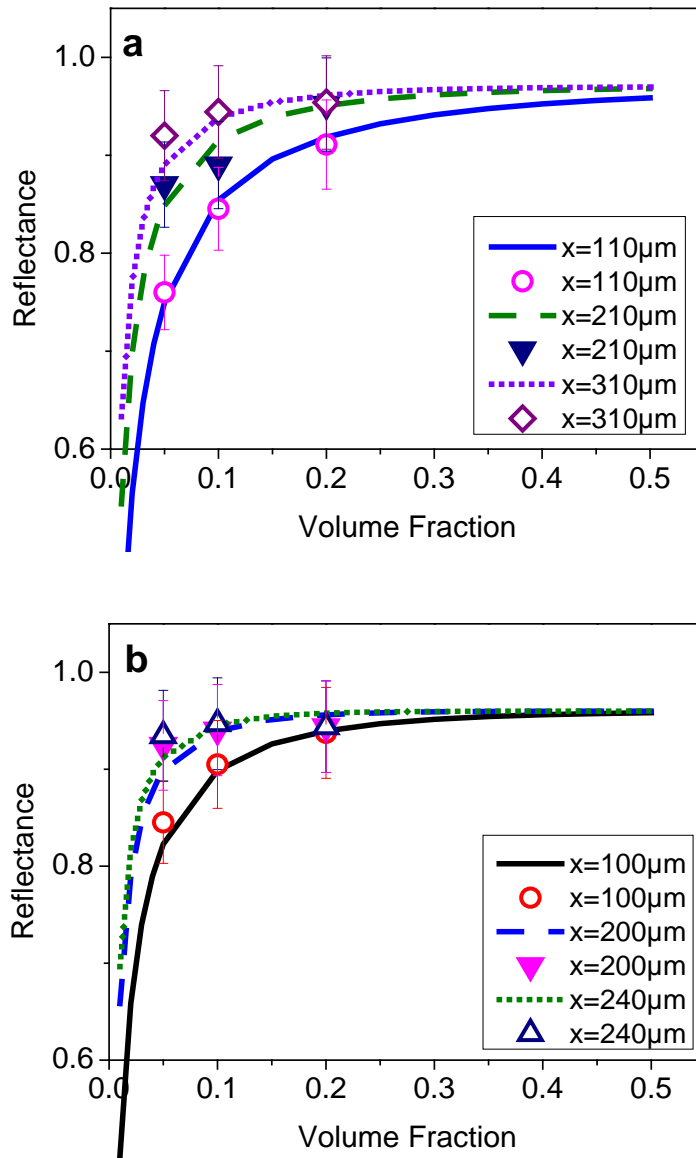


Fig. 3.9. Reflectance vs. filler volume fraction for (a) BN-silicone coatings and (b) ZnO-silicone coatings on Cu substrates at wavelength of 450nm with various thickness. The symbols indicate the measured reflectance at different thickness ( $x$ ) and the lines show the calculated reflectance based on model.

Figure 3.9 presents the reflectance as a function of filler volume fraction for BN-silicone and ZnO-silicone reflectors at wavelength of 450nm. The calculated results are in good agreement with the measurements for all the samples with different thickness. With the same thickness, the reflectance firstly increases as the volume fraction increases from zero to a critical value, and then saturates as the volume fraction continues to increase. The plots indicate that the critical volume fractions for BN and ZnO fillers to effectively reflect incident radiation at 450 nm wavelength are 0.2 and 0.1 for about 200 $\mu$ m thick reflectors. The little deviation in exact value of reflectance could be due to the uncontrolled factors in experimental samples that result in a non-ideal state. However, it still can be seen that the modeling results give us good correlations to determine what filler volume fraction is effective enough for specific fillers at a particular thickness. It is demonstrated from Figs. 3.7, 3.8 and 3.9 that the modeling can be used to determine the critical thickness and filler volume fraction for silicone based reflectors to obtain the maximum reflectance in an approach to reduce the overall weight and manufacturing cost of polymer based reflectors.

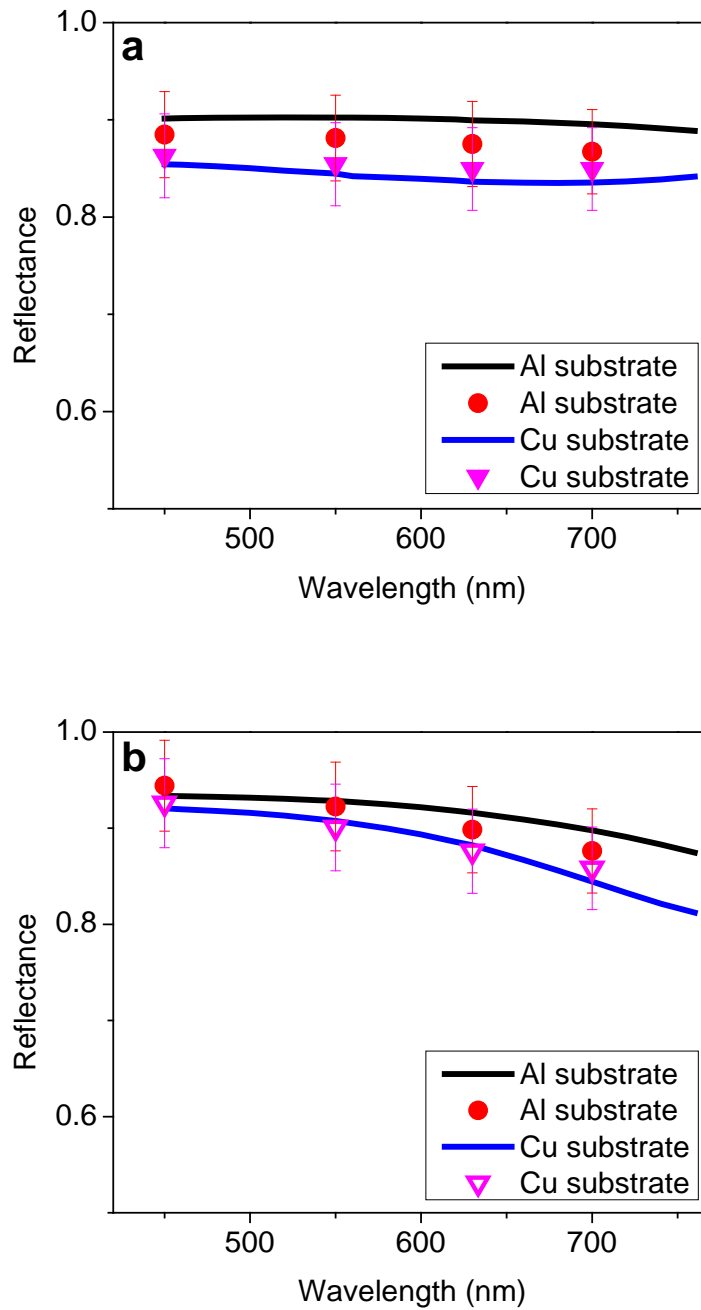


Fig. 3.10. Reflectance of (a) 110  $\mu\text{m}$  thick BN-silicone coatings and (b) 125  $\mu\text{m}$  thick ZnO-silicone coatings on Cu substrate and Al substrate. The filler volume fraction is 0.1. The symbols indicate the measured reflectance at different wavelength and the lines show the theoretical reflectance based on model.

Furthermore, in order to evaluate the capability of this model, we predicted the coating reflectance at different wavelength and compared the results with measurements. The wavelengths measured are 450, 550, 630 and 700 nm, which include the emission peaks of blue, green and red single color LEDs. The comparison curves of the reflectors at selected wavelength are shown in Fig. 3.10. Overall, there is a good agreement between prediction results and experimental data for samples at selected wavelength, indicating the capability of predicting visible light reflectance in our model. We demonstrated that our analytical model presents a useful tool to predict and optimize polymer-filler composite reflectors.

### **3.5. Conclusion**

In this work, we presented a simple analytical model for reflectance of polymer-filler reflector on various substrates by considering the effect of reflector thickness, fillers and back reflection from substrate. This first general analytical results were fully supported by our experimental measurements for the investigation of critical thickness. For the first time, our work, the optimization of reflectors was realized by using the critical thickness of reflector to achieve a theoretical maximum reflectance. Our results indicate the critical thickness can be tailored by controlling the substrate reflection and the filler volume fraction, and our model can be valuable for accelerating the design and optimization of polymer-filler composite reflectors.



## References

1. A. M. K. Dagamseh, B. Vet, P. Šutta and M. Zeman, “Modelling an doptimizaiton of a-Si:H solar cells with ZnO:Al back reflector” *Sol. Energy Mater. Sol. Cells* **94**(12 ), 2119 (2010)
2. Z. Xu, S. Kumar, J. P. Jung and K. K. Kim, “Reflection characterisztics of displacement deposited Sn for LED lead frame” *Mater. Trans.*, **53** (5), 946–950 (2012)
3. S.H. Kee, W..I. Kim, and J.P. Jung, "Reflection characteristics of electroless deposited Sn-3.5Ag for LED lead frames" *Surf. Coat. Tech.*, **235** (25), 778-783 (2013)
4. B. G. Lee, P. Stradins, D. L. Young, K. Alberi, T. Chuang, J. G. Couillard, and H. M. Branz, “Light trapping by a dielectric nanoparticle back reflector in film silicon solar cells” *Appl. Phys. Lett.*, **99**, 064101(2011)
5. T. Chang, C. Liu, W. Lee, and Y. Hsiao, “A study of back electrode stacked with low cost reflective layers for high-efficiency thin-film silicon solar cells” *J. Sol. Energy Eng* **136**(3), 031002 (2014)
6. A. Lin, Y. K. Zhong, S. M. Fu, C. W. Tseng, and S. L. Yan, “Aperiodic and randomized dielectric mirrors: alternatives to metallic back reflectors for solar cells,” *Opt. Express* **22**(S3), A880–A894 (2014)
7. B. Kim, J. Kim, W. Ohm, and S. Kang, “Eliminating hotspots in a multi-chip LED array direct backlight system with optimal patterned reflectors for uniform illuminance and minimal system thickness” *Opt. Express* **18**(8), 8595–A8603 (2010)
8. A. B. Starry, “Diffuse reflective article” US 7,660,040 B2 (2010)
9. C. J. Kaminsky, R. P. Bourdelais, “Light reflector with variable diffuse light reflection” US 0214718 A1 (2003)

10. C.-C. Chen, C.-Y. Wu, and T.-F. Wu, "LED back-light driving system for LCD panels," in Proc. Appl. Power Electron. Conf., 381–385 (2006)
11. C. Pan, C. Su, H. Cheng, and C. Pan, "Backlight module and brightness enhancement film thereof" US 7290919 B2 (2007)
12. Y. Shao, Y. Shih, G. Kim and F. G. Shi, "Study of optimal filler size for high performance polymer-filler composite optical reflectors" Opt. Materials Express, **5**(2), 423-429 (2015)
13. <http://refractiveindex.info/>
14. W. Qiu, "PDMS Based Waveguides For Microfluidics And EOCB" M. S., Zhejiang University (2006).
15. S. A. Ackerman and G. L. Stephens. "The Absorption of Solar Radiation by Cloud Droplets: An Application of Anomalous Diffraction Theory" J. Atmos. Sci., **44**(12), 1574–1588 (1987)
16. H. C. van de Hulst, *Light scattering by small particles* (John Wiley and Sons, 1957).
17. A. Kokhanovsky and E. Zege, "Optical properties of aerosol particles: a review of approximate analytical solutions" J Aerosol Sci., **28** (1), 1-21 (1997)
18. D. L. Mitchell, A. J. Baran, W. P. Arnott, and C. Schmitt, " Testing and Comparing the Modified Anomalous Diffraction Approximation" *J. Atmos. Sci.*, **63** (11), 2948–2962 (2006)
19. C.F. Bohren, D. Huffman, *Absorption and scattering of light by small particles* (John Wiley and Sons, 1983).
20. P. Kubelka, "New contributions to the optics of intensely light-scattering materials. Part I," J. Opt. Am. **38**(5), 448–457 (1948)

## **CHAPTER 4:**

# **EFFECT OF FILLERS ON SILICONE-BASED DIFFUSE REFLECTIVE FILMS FOR BACKLIGHT UNITS**

### **4.1. Introduction**

High reflectivity in visible spectra is critical in many lighting applications such as LED wall lights, flood lights and area lights [1-5]. In contrast to specular reflection where light is only reflected at an angle equal to that of the incident light, diffuse reflection is able to reflect light at multiple angles providing an even distribution of light from the surface. Therefore, diffuse reflectors are preferable for LCD and LED backlight displays in order to improve uniformity and brightness of light distribution, eliminate hotspots for better overall optical aesthetics, and reduce the energy consumption [6-9].

Additional requirements on backlight reflectors are also needed for some special applications. For backlights used in portable devices such as laptops and cell phones, the reflective materials are required to be used as thin films, for example, less than 250 microns [10], in order to minimize the thickness of the whole display illumination systems. For direct view backlight, the reflective materials are required to have high visible light reflectance, high stability under the operation temperature in the range of 50 to 70°C, and good stability to humidity [10].

Currently, many high quality commercial diffuse reflectors are very expensive and only available in standard shapes, such as white inorganic compounds in the form of pressed cake or ceramic tile, microporous materials made from sintered polytetrafluoroethylene (PTFE) [11],

microporous materials with thermally induced phase separation technology [12], and microvoided materials filled with particles and controlled air voids [13], etc. Other commercial diffuse reflectors employ complicated manufacturing methods to control the surface shape, such as reflectors with concave-convex surface formed by deposition and patterning the insulating film [14], reflectors with surface pattern formed by contacting with a chill roller, and reflectors with complex and random three-dimensional structures created by exposure to radiation [15], etc. All these commercial products require manufacturing methods which are time consuming and cost prohibitive. Therefore, the objective of this work is to develop high reflectance but inexpensive and easy to produce diffuse reflective thin films.

Silicone-based diffuse reflective films, where white inorganic fillers are incorporated into silicone matrices, are inexpensive and improved options for LED and LCD backlights. Such diffuse reflective films provide high reflectance in visible light range, excellent stability under thermal and radiation, as well as adequate reflection performance with reduced thickness. Moreover, high reflectance silicone based reflectors require no complicated fabrication technique, thus they are much more cost effective than many other expensive commercial products mentioned above.

There are many studies conducted on dielectric diffuse reflectors, such as white polystyrene microsphere film and electrospun nanofiber web[17, 18], but very few reports on silicone based reflective thin films used in backlight unit. In this study, the effect of fillers on silicone-based reflective films were investigated and their optical properties and environmental stability were experimentally examined. The results provide an important guidance for the structural design in silicone-based reflector manufacturing and development of cost effective thin diffuse reflective films for backlight unit applications.

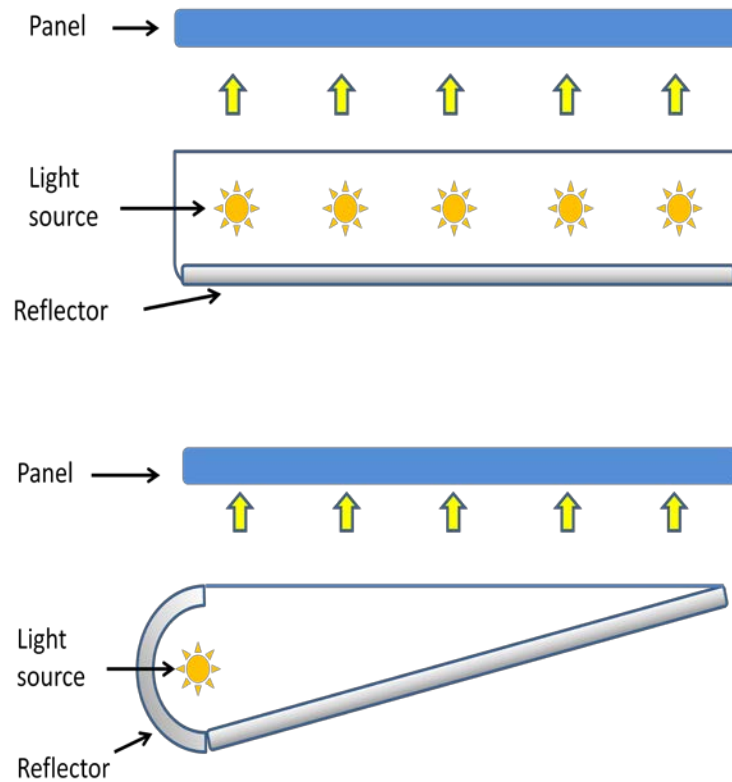


Fig. 4.1 Structures of (upper) direct-type backlight and (lower) edge-type backlight.

## 4.2. Experiment

### 4.2.1 Fabrication of reflective films

#### 4.2.1.1 Materials

In the experiment, silicone-based diffuse reflective films were fabricated by mixing transparent silicone resin with inorganic fillers. The inorganic fillers used for samples are Al<sub>2</sub>O<sub>3</sub> (from Inframat Advanced Materials Inc), TiO<sub>2</sub>, BN (from Sigma-Aldrich), ZnO (from Inframat Advanced Materials Inc), MgO and SiO<sub>2</sub> powders. The properties of materials used in polymer-filler reflectors are listed in Table 4.1.

Table 4.1. Properties of materials used for reflectors

	Silicone resin	Al <sub>2</sub> O <sub>3</sub> powders	TiO <sub>2</sub> powders	ZnO powders	BN powders	SiO <sub>2</sub> powders
Refractive index (λ=450nm)	1.41	1.78	2.81	2.11	1.81	1.47
Density (g/cm <sup>3</sup> )	1.03	3.95	4.23	5.61	2.1	2.65
Average filler size (μm)	-	1	0.2	1	1	1

#### 4.2.1.2 Mixing

In order to form a homogenous mixture, various amounts of filler were mixed with high performance silicone using a Shinky high shear mixer at 2500 r/min for 5 minutes.

#### 4.2.1.3 Degassing

After mixing, the composites were degassed under a vacuum of 10<sup>-2</sup> Pa for 30 minutes in order to get rid of the trapped air bubbles.

#### 4.2.1.4 Curing

The mixture was coated on to PTFE substrates using film applicator and cured at 150°C for 2 hours, and then carefully detached the cured films from substrates.

#### 4.2.2 Reflectance measurement

The light reflectance of the fabricated reflectors at a wavelength range from 400 to 800 nm was measured using a conventional light reflectometer (Filmetrics Model F20).

#### 4.2.3 Reliability test

The following aging conditions have been used to simulate the environment for silicone based reflectors used in backlight units:

- a. High temperature test: high temperature at 150°C for 500 hours
- b. High temperature/ humidity test: high temperature at 85°C and humidity at 85% RH for 500 hours

The following aging conditions have been used to simulate the environment for silicone based composites and commercial epoxy based composites used in general electronic packaging:

- c. Combined thermal and radiation aging test: blue radiation at 150°C for 1080 hours and UV radiation at 150°C for 24 hours. For blue-radiation aging test, all samples were exposed to a blue light with a light density of 994718 W/m<sup>2</sup>. For UV-radiation aging test, all samples were exposed to a UV light with a power of 200W and placed at different distances from the lamp to adjust the radiation density.

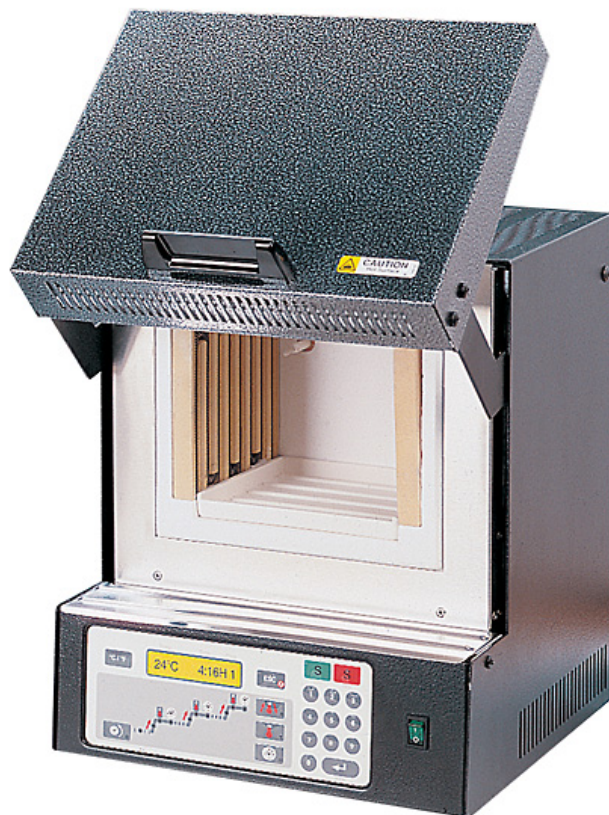


Fig. 4.2. Vulcan programmable furnace for high temperature thermal aging.





Fig. 4.3 ChemKorea temperature and humidity chamber used for high temperature/ humidity  
test

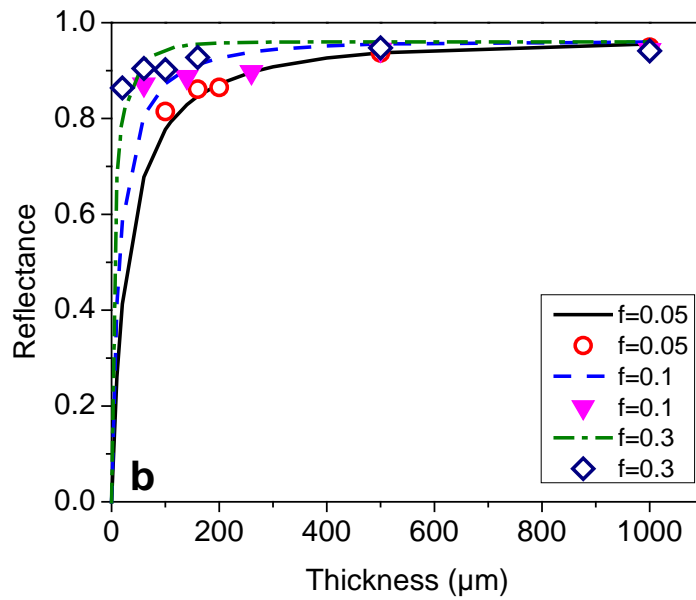
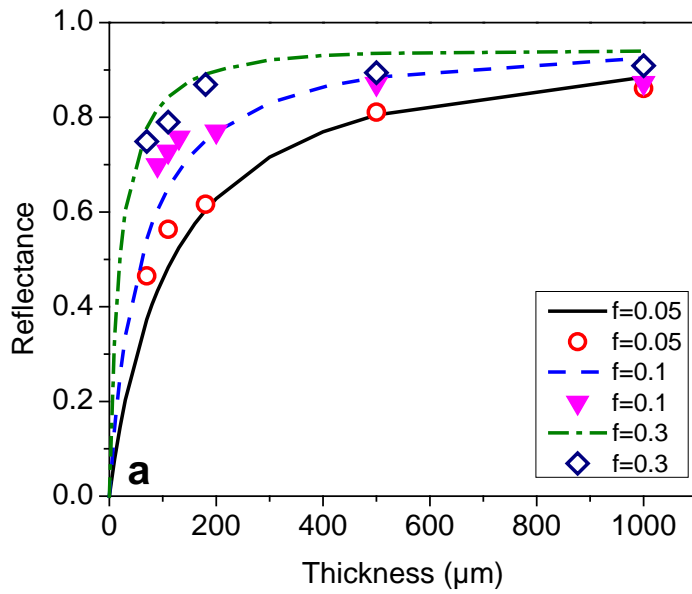
### 4.3. Light reflectance

For backlights used in portable devices, the reflectors are required to have high levels of reflection of visible light from very thin materials. Also, it is desirable to have large amount of diffuse reflectance across the reflection film, to compensate for uneven brightness across a backlit display. Therefore, much efforts are required to develop thin reflective films or coatings with high diffuse reflection.

A good understanding of light scattering dependence on the above-mentioned parameters in polymer-filler composites is an essential prerequisite for optimization and design of thin reflective films. The key parameters are thickness, volume fraction, the refractive index difference between particles and matrix, and the reflectivity of filler materials.

#### 4.3.1.1 Reflectance of silicone composites

In this study, the reflectance of the silicone composites filled with various inorganic fillers was predicted using our analytical model described above. In order to verify the model, we prepared the silicone composites filled with  $\text{Al}_2\text{O}_3$ ,  $\text{TiO}_2$  and  $\text{ZnO}$ , and measured their reflectance to compare with model prediction.



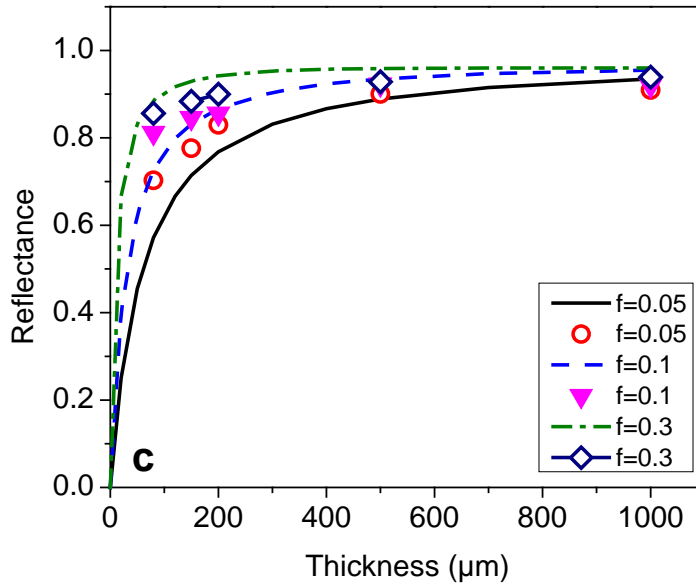


Fig. 4.4 Reflectance vs. reflector thickness for (a)  $\text{Al}_2\text{O}_3$ -silicone composites, (b)  $\text{TiO}_2$ -silicone composites and (c)  $\text{ZnO}$ -silicone composites at wavelength of 450nm with various thickness. The symbols indicate the measured reflectance with different filler volume fraction ( $f$ ) and the lines show the theoretical reflectance based on model.

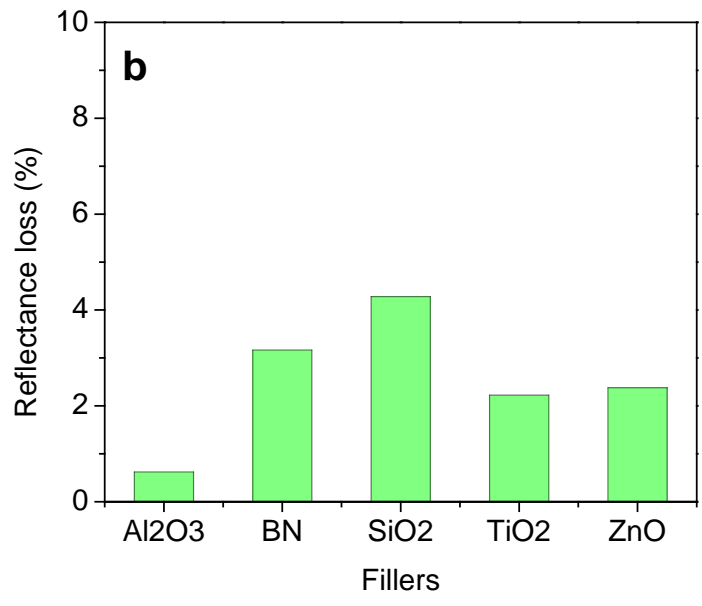
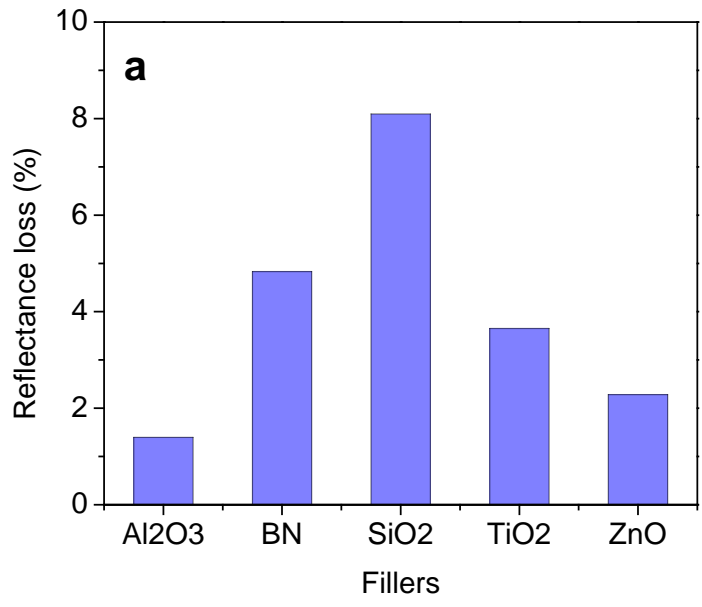
The comparison between calculated results and measured reflectance as a function of reflector thickness for  $\text{Al}_2\text{O}_3$ -silicone and  $\text{TiO}_2$ -silicone reflectors is shown in Figure 4.4. All the reflectances are taken at wavelength of 450nm, which is the emission peak of blue LED chips. The theoretical results are in a good agreement with experimental data, verifying the optimization trends calculated by the modeling. It is shown in the figure that a non-linear relationship between reflectance increase and thickness of reflector exist. For both types of reflectors, the reflectance increases rapidly from very small thickness to a critical thickness, and then reaches stabilization as the reflector getting thicker. The scattering interfaces between fillers

and matrix within the composite reflectors increases as total thickness increases, resulting in a boost of reflectance for reflectors until it reaches the saturation value. By using the optimal filler size predicted by model [16] and high volume fraction, the 200  $\mu\text{m}$ -thick silicone composite film can achieve a reflectance higher than 0.9. It can be seen that the modeling results give us good correlations to determine what filler volume fraction is effective enough for specific fillers at a particular wavelength. It is demonstrated that the modeling can be used to determine the critical parameters for silicone based reflectors to obtain high reflectance ( $>0.9$ ) with a reduced thickness for backlights application.

#### **4.4. Reliability**

##### 4.4.1 High temperature reliability

The yellowing and the shorter lifetime are the most severe problems for polymeric reflective materials in high-power LED and LCD backlights units. In high-power device packages, large amounts of heat generated and accumulated inside the package, leading to a thermal degradation of reflector cups around blue LED chips [9]. In this paper, we chose five most commonly used white fillers:  $\text{Al}_2\text{O}_3$ ,  $\text{TiO}_2$ , BN, ZnO and  $\text{SiO}_2$ , and studied the reflectance loss of silicone composites filled with these fillers by comparing the initial state and after high temperature aging test.



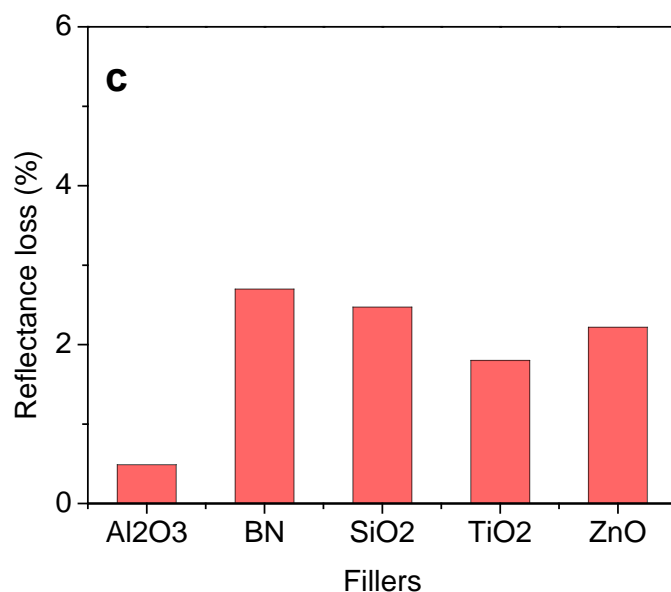
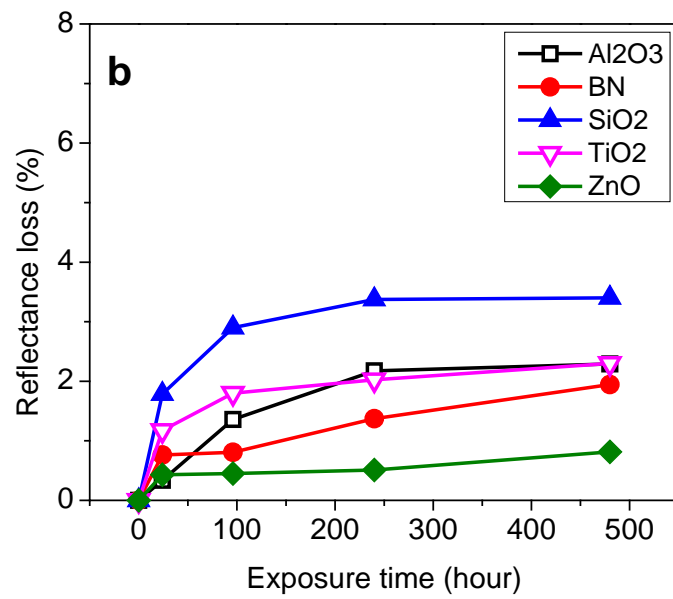
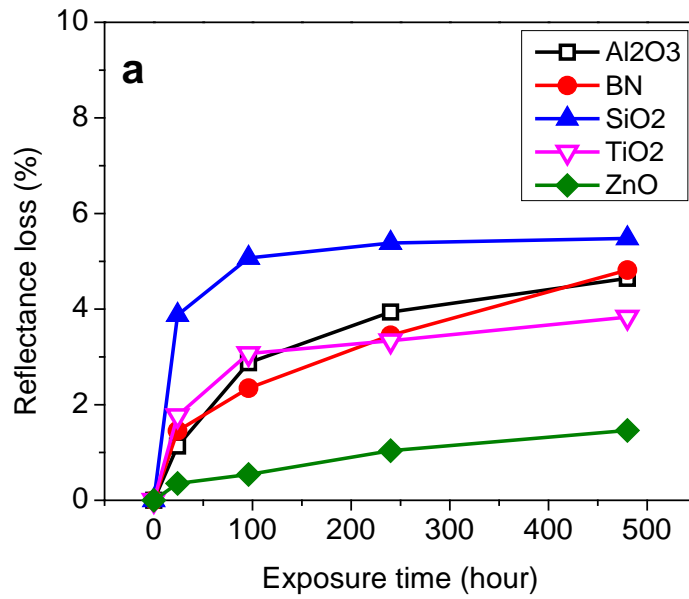


Fig. 4.5 Reflectance loss of silicone reflective films filled with Al<sub>2</sub>O<sub>3</sub>, TiO<sub>2</sub>, BN, ZnO and SiO<sub>2</sub> under 150°C aging for 500 hours at (a) 450nm, (b) 550nm and (c) 630nm wavelength.

Figure 4.5 shows the loss of reflectance silicone reflective films filled with Al<sub>2</sub>O<sub>3</sub>, TiO<sub>2</sub>, BN, ZnO and SiO<sub>2</sub> under 150°C aging for 500 hours. The change in reflectance loss at 450nm wavelength is shown in Figure 4.5 (a). After 500 hours thermal aging, the SiO<sub>2</sub> composite samples experienced a 8.3% loss in reflectance along with the slight cloudiness and yellowing phenomenon, while Al<sub>2</sub>O<sub>3</sub> composite samples showed only 1.4% loss with almost no change in colors. Figure 4.5 (b) shows the loss of reflectance at 550nm wavelength. The reflectance loss of Al<sub>2</sub>O<sub>3</sub> composite samples are less than 1% , while SiO<sub>2</sub> composite samples still suffers the highest reflectance loss at about 5%. At 630 nm wavelength, Al<sub>2</sub>O<sub>3</sub> composite samples still are the most thermally stable ones. Overall, the thermal stability for silicone composite reflectors are Al<sub>2</sub>O<sub>3</sub> > TiO<sub>2</sub> > ZnO > BN > SiO<sub>2</sub>. These degradation of silicone composite reflectors cause insignificant loss of brightness and uniformity of backlights.

#### 4.4.2 High temperature and humidity reliability





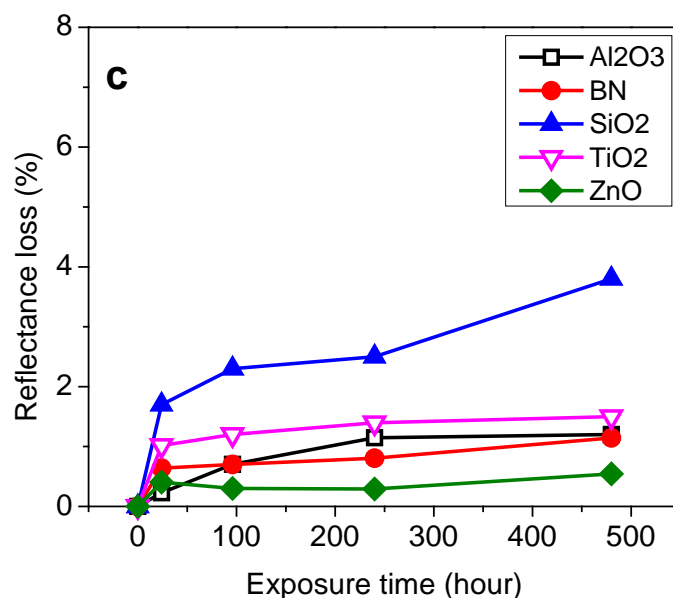
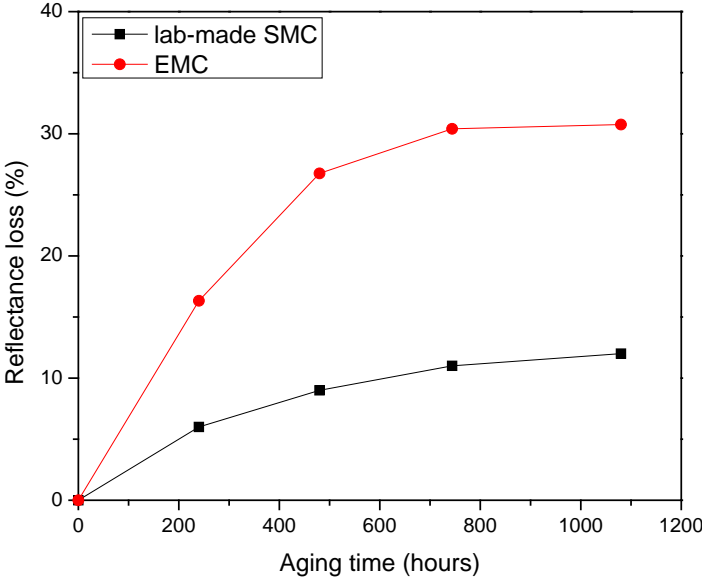


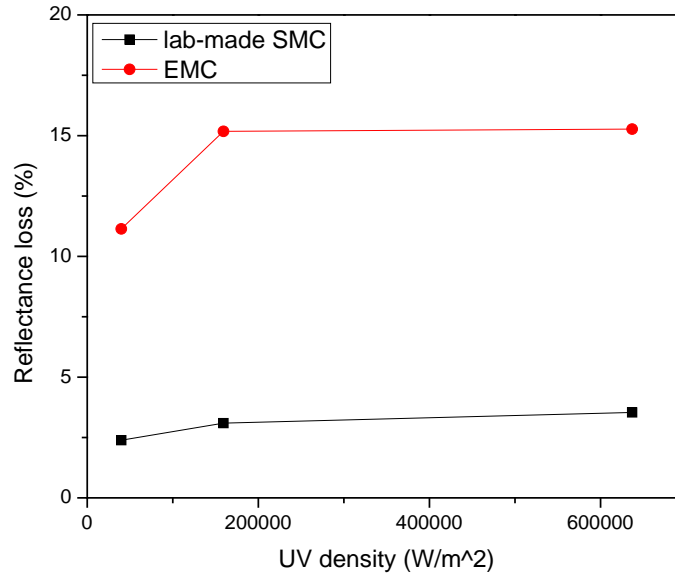
Fig. 4.6 Reflectance loss of silicone reflective films filled with Al<sub>2</sub>O<sub>3</sub>, TiO<sub>2</sub>, BN, ZnO and SiO<sub>2</sub> under high temperature at 85°C and humidity at 85% RH for 500 hours at (a) 450nm, (b) 550nm and (c) 630nm wavelength.

Most polymeric reflective materials suffer degradation during the exposure to high temperature and moisture. Figure 4.6 represents the loss of reflectance of silicone reflective films filled with Al<sub>2</sub>O<sub>3</sub>, TiO<sub>2</sub>, BN, ZnO and SiO<sub>2</sub> under 85°C /85% RH aging conditions. At 450, 550 and 630 nm wavelengths, silicone reflective films filled with ZnO show the smallest reflectance loss, but silicone reflective films filled with SiO<sub>2</sub> show the largest loss. The filler dependent stability of thermal and humidity for silicone composite reflectors is: ZnO >TiO<sub>2</sub> > Al<sub>2</sub>O<sub>3</sub> >BN >SiO<sub>2</sub> at 450nm, ZnO >TiO<sub>2</sub> > Al<sub>2</sub>O<sub>3</sub> >BN >SiO<sub>2</sub> at 550nm, and ZnO >TiO<sub>2</sub> > Al<sub>2</sub>O<sub>3</sub> >BN >SiO<sub>2</sub> at 630nm. All the silicone composite samples experience a reflectance loss less than 6% with almost no change in color, demonstrating a good thermal and moisture resistance.

The silicone composites present not only good thermal and moisture stability, but also superior UV and blue radiation resistance than the common polymer based materials, such as epoxy molding composites, which is widely used for electronic packaging materials.



(a)



(b)

Fig. 4.7. Reflectance loss of commercial EMC and lab-made SMC under (a) 994718 W/m<sup>2</sup> blue radiation + 150°C aging for 1080 hours and (b) UV radiation + 150°C aging for 24 hours

Figure 4.7 (a) shows the loss of reflectance for commercial epoxy molding composites (EMC) and lab-made silicone molding composites (SMC) samples after 1080 hours thermal and blue-radiation aging. The reflectance loss of SMC samples are only 12% while EMC samples still suffer severe reflectance loss at about 31%. Figure 4.7 (b) shows the loss of reflectance for commercial EMC and lab-made SMC samples after 24 hours combined thermal aging and UV-radiation with different radiation density. One can see that lab-made SMC has a very low sensitivity to blue and UV radiation. In general, the mechanisms of radiation aging and thermal aging are different from the initiation process. The initiation of thermal oxidation is the thermal decomposition of chemical bonds in the polymer, however, radiation aging is initiated via energy absorption by chromophores and then chemical bonds breaking during the change of energy

states [9]. Compared with the organic carbon-oxygen (C-O) bond (339KJ/mol) in epoxy structure, the higher bond energy of inorganic siloxane (Si-O) bond (444KJ/mol) makes silicone structure more stable and possess a better thermal and radiation resistance in order to withstand with heat generation and high energy. Because of the presence of aromatic functional group, commercial EMC samples suffer more reflectance loss under the combined aging test and produces an initial drop of 28% over the first 500 hours. Conversely, the lab-made SMC samples have so far demonstrated relatively small reflectance change and almost no visual signs of degradation under all these aging tests. It is very likely that they will continue to perform well with longer exposure time and higher radiation density.

#### **4.5. Conclusion**

In this study, we use analytical model to investigate the thin polymer-filler reflective films for LCD and LED backlights. A good agreement was found between theoretical results and experimental data. It is demonstrated that the modeling can be used to optimize silicone based reflectors to obtain high reflectance ( $>0.9$ ) with a reduced thickness for backlights application. Besides, the filler dependent high temperature and moisture stability of silicone composite reflectors were investigated. Silicone reflective films filled with ZnO show the best stability, while silicone reflective films filled with SiO<sub>2</sub> show the worst. It is also demonstrated that Silicone based packaging materials are expected to perform well with longer exposure time and higher radiation density. Our results provide an important guidance for the design in polymer-filler reflector manufacturing and development of thin polymer-filler reflective films for backlight unit application.

## References

1. B. Curtin, R. Biswas, and V. Dalal, "Photonic crystal based back reflectors for light management and enhanced absorption in amorphous silicon solar cells," *Appl. Phys. Lett.* **95**(23), 231102 (2009)
2. Leung, S, Zhang, Q. Xiu, F. Yu, D. Ho, J. C. Li, D. Fan, Z. "Light Management with Nanostructures for Optoelectronic Devices." *J. Phys. Chem. Lett.* **5**,1479-1495 (2014)
3. R. H. Horng, C. C. Chiang, H. Y. Hsiao, X. Zheng, D. S. Wu, and H. I. Lin, "Improved thermal management of GaN/sapphire light-emitting diodes embedded in reflective heat spreaders." *Appl. Phys. Lett.* **93**, 111907 (2008)
4. G. T. Valliath, Z. A. Coleman, J. L. Schindler, R. Polak, R. B. Akins and K. W. Jelley, "Design of Hologram for Brightness Enhancement in Color LCDs." *SID Symposium Digest of Technical Papers*, **29**,1139–1143 (1998)
5. J. K. Kim, T. Gessmann, E. F. Schubert, J. Q. Xi, H. Luo, J. Cho, C. Sone, and Y. Park, "GaInN light-emitting diode with conductive omnidirectional reflector having a low-refractive-index indium-tin oxide layer," *Appl. Phys. Lett.* **88**(1), 013501 (2006)
6. K. Kälantär , S. Matsumoto , and T. Onishi , " Functional light-guide plate characterized by optical micro-deflector and micro-reflector for LCD backlight," *IEICE Trans. Electron.* **E84-C** , 1637 – 1646 ( 2001 )
7. Anderson, J., Schardt, C., Yang, J., Koehler, B., Ostlie, B., Watson, P., Ingham, K., Kienitz, S. and Ouder Kirk, A. "New Back Reflector and Front Film for Improved Efficiency of Direct-lit LED Backlights for LCD TV." *SID Symposium Digest of Technical Papers*, **38**: 1236–1239 (2007)

8. Mi-Yeon Yu, Byung-Woo Lee, Jeong-Ho Lee, and Jae-Hyeon Ko, "Correlation Between the Optical Performance of the Reflective Polarizer and the Structure of LCD Backlight," *J. Opt. Soc. Korea* **13**, 256-260 (2009)
9. C. Pan, C. Su, H. Cheng, and C. Pan, "Backlight module and brightness enhancement film thereof" US 7290919 B2 (2007)
10. W. G. O'Brien, "Diffuse reflector, diffuse reflective article, optical display, and method for producing a diffuse reflector." US 20100014164 A1
11. J. Masuda, M. Ohkura, S. Tanaka, R. Morita, and H. Fukushima, "Microporous polypropylene film and process for producing the same." US 8491991 B2
12. W. Kretman, S. Kayter, Diffuse reflective articles, US6497946B1
13. W. Ing, W. Hou, "Lighting device, display, and method for manufacturing the same." US20110006316A1
14. E. Mizobata, H. Ikeno, and H. Kanoh, "Reflective LCD having a particular scattering means." US6018379 (2000)
15. P. R. Fleming, A. J. Ouderkirk, E. J. Borchers, "Method and apparatus for step and repeat exposures." US6285001 B1 (2001)
16. Y. Shao, Y. C. Shih, G. W. Kim and F. G. Shi, "Study of optimal filler size for high performance polymer-filler composite optical reflectors." *Opt. Mater. Express*, **5**, 423–429 (2015)
17. M. Wang, X. Ye, X. Wan, Y. Liu, and X. Xie, "Brilliant white polystyrene microsphere film as a diffuse back reflector for solar cells." *Mater. Lett.*, **148**, 122-125 (2015)

# **CHAPTER 5:**

## **PASSIVE COOLING ENABLED BY NOVEL POLYMER COMPOSITE COATING**

### **5.1 Introduction**

Thermal control coating materials with high cooling effect are critical in many applications such as energy conversion and a wide variety of future micro- and nano-technologies [1-3]. Passive radiation cooling refers to a process in which a subject will emit as radiation heat energy absorbed through normal convection and conduction process. Heat dissipation through radiation has its advantage in being passive, and no power supply is required and thus ideal for space sensitive micro- and nano-devices [4-6]. Also, the passive cooling shows the possibility for water-free and electricity-free approaches to cooling building and vehicles at all hours of the day to decrease the carbon emissions caused by air conditioning [3].

Key parameters in determining the radiation cooling potential of a polymer composite coating is the type of filler, filler size and thickness of coating [5,7-8]. Recent reports [9-10] suggest that the radiation cooling is greatly enhanced if the carbon filler is used with its size in the range of a few tens of nanometers due to quantized lattice motion. Many researchers study thermal cooling coatings only focusing on the reflectivity and emissivity of coatings in infrared region [11-13]. In real applications, the apparent cooling effect is the most important factor for cooling coatings to improve energy efficiency and offer financial and environmental benefits.

However, in view of the significance, both technologically and scientifically, it is surprisingly to find that there is no report on a systematic investigation on the filler size and thickness dependence of the apparent cooling effect of polymer-filler composites.

The objective of this work is to provide such a first investigation. Three types of fillers, including  $\text{Al}_2\text{O}_3$ ,  $\text{TiO}_2$  and  $\text{ZnO}$  are included in the investigation, with the filler size ranging from nanometers to micrometers, and the polymer matrix used in the study is optical clear silicone because of its superior thermal and radiation stability. The thicknesses of coatings studied are from 40 to 360 microns. The cooling effect dependence on the filler type is found to be in the order of  $\text{Al}_2\text{O}_3 > \text{TiO}_2 > \text{ZnO}$ . It is established experimentally for the first time that the radiation cooling exhibits a very weak filler size dependence. Thus, contrary to prior reports [1,9-10], the so-called molecular fan, i.e., radiation induced cooling by using a polymer composite coating with filler size less than a few tens of nanometers, might be unnecessary to provide the maximum cooling effect. Since the effect of filler size on apparent cooling effect of polymer-filler composites is insignificant, it is much easier for the manufacturer to select filler particle size according to specific applications and requirements without compromising cooling effects.

## **5. 2. Experiment**

### **5.2.1 Sample preparation**

The fillers used are  $\text{Al}_2\text{O}_3$  (from Inframat Advanced Materials),  $\text{ZnO}$  (from Noah Technology) and  $\text{TiO}_2$  (from Inframat Advanced Materials), which are selected because of their relatively high infrared emissivity values: 0.90-0.95 for  $\text{Al}_2\text{O}_3$ ,  $\text{ZnO}$  and  $\text{TiO}_2$  white coatings. As shown in Fig. 1, the diameters of the  $\text{Al}_2\text{O}_3$  fillers are 0.04, 0.1, 1 and 10 micron, the diameters of the  $\text{TiO}_2$  fillers are 0.04, 0.1, 5 and 44 micron, the diameters of the  $\text{ZnO}$  particles are 0.1, 0.14, 1 and 44 micron. The polymer resin selected for making polymer-filler composite is a



polysilicone from Dow Corning, which is selected because of its good chemical stability, and superior thermal and UV resistance.

The radiation cooling enabled by the polymer-filler composite which is prepared by mixing silicone resin with various amounts of filler using a Shinky high shear mixer at 2500 r/min for 5 minutes. After mixing, the composite was degassed under a vacuum of  $10^{-2}$  Pa for 30 minutes to get rid of the trapped air bubbles. The mixture was then coated onto polished aluminum (Al) plates and cured at 150°C for 2 hours. The dimensions of Al plates are 50 mm × 50 mm × 1mm. An uncoated-Al plate is used as a control specimen (baseline) to evaluate the improvement in the heat dissipation of the composite layer.

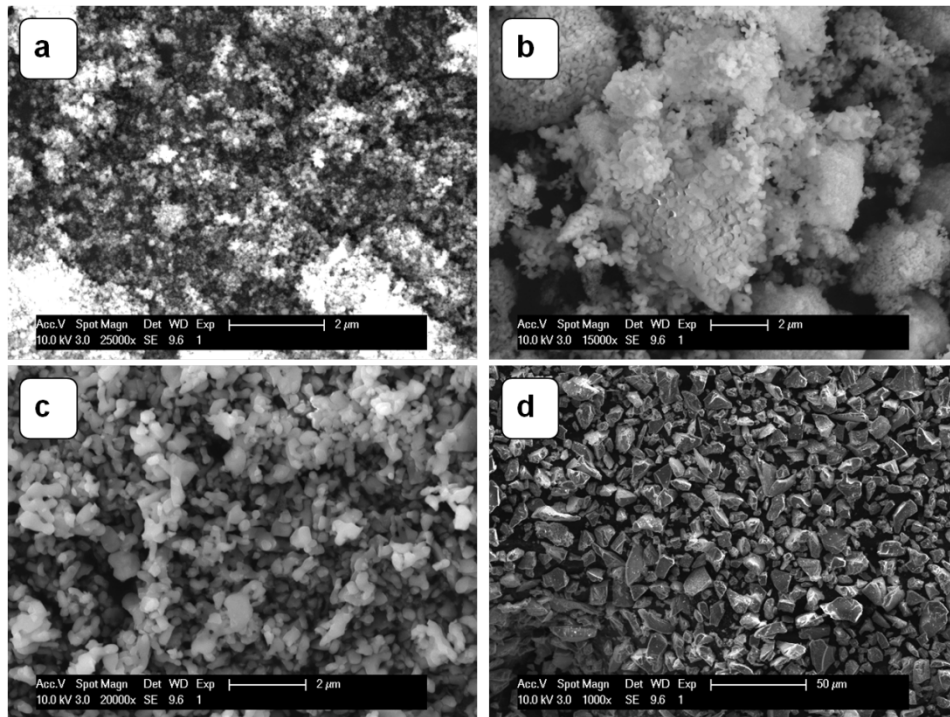


Fig. 5.1 SEM images of Al<sub>2</sub>O<sub>3</sub> fillers at size of (a) 40nm, (b) 100nm, (c) 1 micron and (d) 10microns.

### 5.2.2 Experiment set up

The cooling effect is determined by comparing the decrease in surface temperature of the coating specimens with respect to the baseline by following the same reported experimental set up and procedure [1, 10]. The main part of the system consists of a heating platform, the schematic of which is shown in Fig.5.2. The specimen (coated-Al plate) was heated by mounting it in contact with the upper surface of the copper disk which is heated by the cartridge heater. A good thermal contact was formed between the specimen and the copper disk by tightening the screws. The heating system is set up inside a glass shield where we can consider the effect of convection to be equal for all the specimens. The surface temperature of the specimen is directly measured by thermometer (Omega, model CL3515R). In this experiment, the cartridge heater is operated at two power levels: 9 W and 25 W. Two K-type thermocouples are used to measure the surface temperature of the board and that of the coating, respectively. It takes about 180 minutes for the temperature of the whole system to reach a steady state. The whole heating system is placed in a glass box without forced air flow. The ambient temperature is kept at 23 °C.

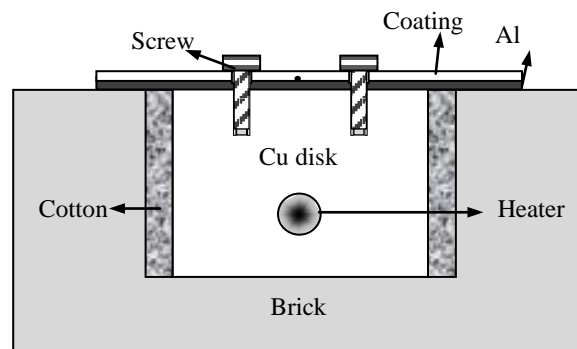
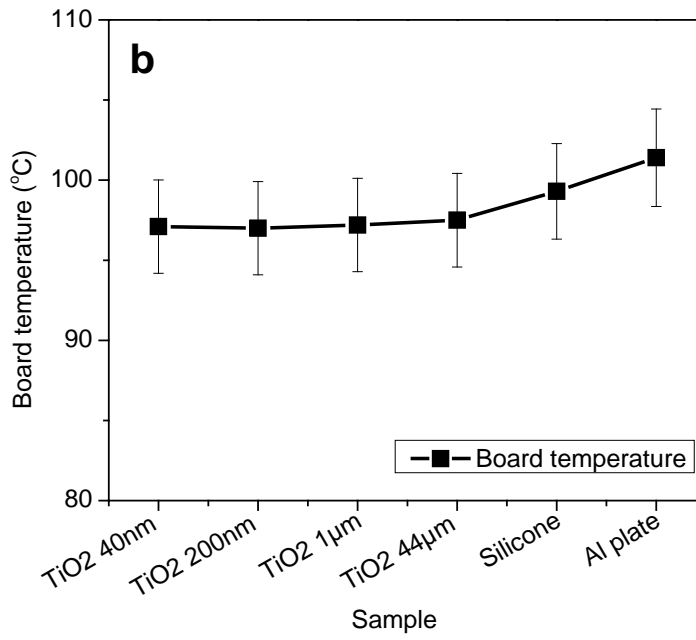
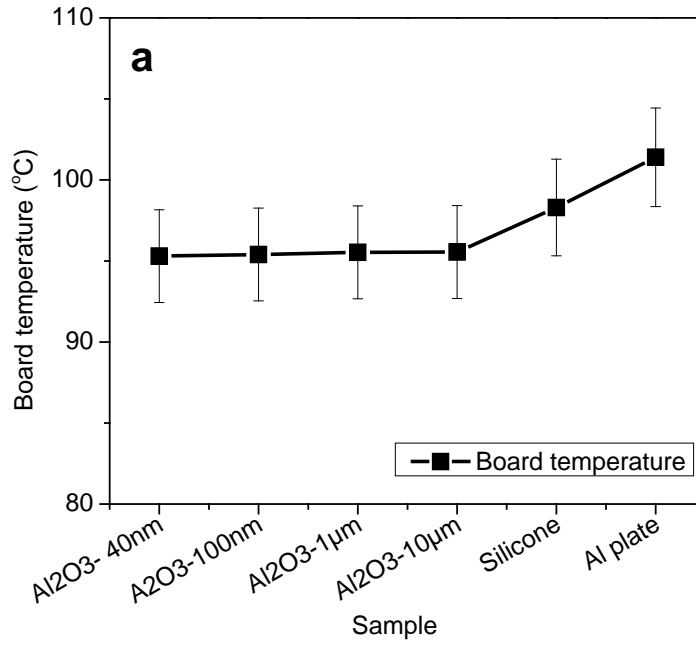


Fig. 5.2 Schematic drawings of heating system

### 5.3. Result and Discussion

The dependence of the cooling effect, i.e., the temperature reduction of the coating surface on filler size is presented in Fig. 5.3 for three different fillers,  $\text{Al}_2\text{O}_3$ ,  $\text{TiO}_2$ , and  $\text{ZnO}$ . For all the experiments, the filler volume fraction is 0.1 and the polymer-filler coating layer has a thickness of  $70\pm 5$  microns. The inserts show the same data with the filler sizes at a logarithmic scale. It is evident that the surface temperature of the Al plate is effectively reduced by the polymer-filler coating layer.



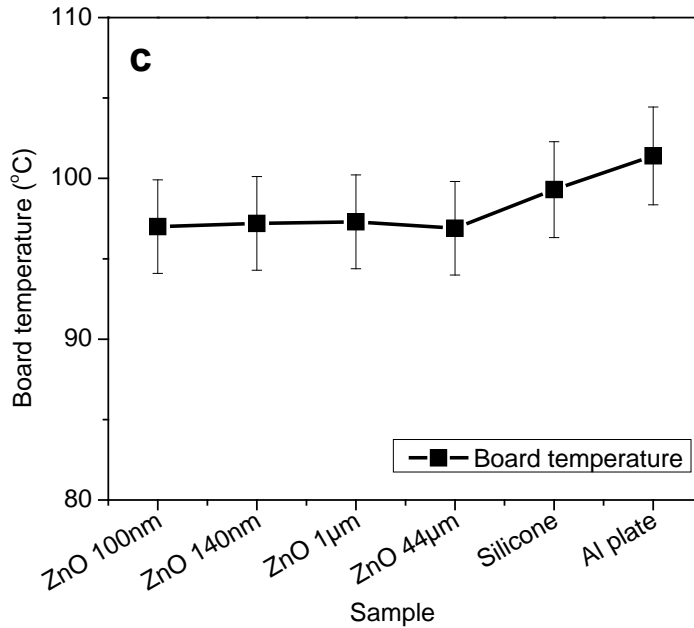


Fig. 5. 3 Board temperature of (a)  $\text{Al}_2\text{O}_3$ , (b)  $\text{TiO}_2$  and (c)  $\text{ZnO}$  composites coatings as a function of filler size. The filler volume fraction is 0.1 and the coating thickness is  $70\pm 5$  microns. The input power is fixed at 9 Watts.

Figure 5.3 shows the measured board temperature of different coating specimen at 9 W power levels. All of the  $\text{Al}_2\text{O}_3$ ,  $\text{ZnO}$  and  $\text{TiO}_2$  composite coatings have a filler volume fraction of 0.1. It is shown that the surface temperature of the board is reduced by application of studied coatings, from pure is 101.4 °C. The application of silicone,  $\text{Al}_2\text{O}_3$ ,  $\text{TiO}_2$  and  $\text{ZnO}$  composite coatings, the board temperature was reduced to 98.3, 96, 97 and 97.3 °C, respectively. The trend of the cooling effect exhibit an insignificant dependence on filler size for three types of polymer-filler coatings. The differences of board temperatures for different filler sizes are less than 1.5 °C for the case of  $\text{Al}_2\text{O}_3$ ,  $\text{TiO}_2$  and  $\text{ZnO}$  fillers.

Theoretically, there is a strong filler size dependence on emissivity as reported in reference 14 and 15. The emissivity of the surface is its effectiveness in emitting energy

as thermal radiation. When the filler size becomes very small, the maximum wavelength of the thermal emission is order of the size, so that the spectrum of the thermal emission becomes different compared to well-known blackbody radiation. As the filler size increases, the normalized emissivity ( $I$  of filler /  $I$  of blackbody) increases sharply as shown in Fig. 5.4 from Ref. 15. However, the apparent cooling performance of silicone composites observed in our study didn't present such filler size dependence.

The cooling effect for fillers in different sizes might be resulted from the combined effect of filler emissivity and conduction. Nano and submicron size fillers, which are much smaller than the lower limit of the NIR wavelength range, require much higher minimum energy to be excited, and corollary have much lower radiation density and emissivity compared [14]. For micrometer size fillers, which are equal or larger than NIR and IR wavelengths, their energy density and emissivity slowly increases as the filler size increases and gradually approaches 1 at which the energy density of filler radiation is equal to that of blackbody radiation [14]. On the other hand, the smaller filler size, the higher the ratio of surface atoms to total atoms, which leads to a higher degree of interaction and larger surface areas, as shown in Fig. 5.5 It has been reported that with a given filler volume fraction, the smaller the particle size, the higher the composite's thermal conductivity would be [16]. Therefore, the combination of radiation emissivity and thermal conduction lead to a stable cooling effect for composites embedded with fillers in different sizes.

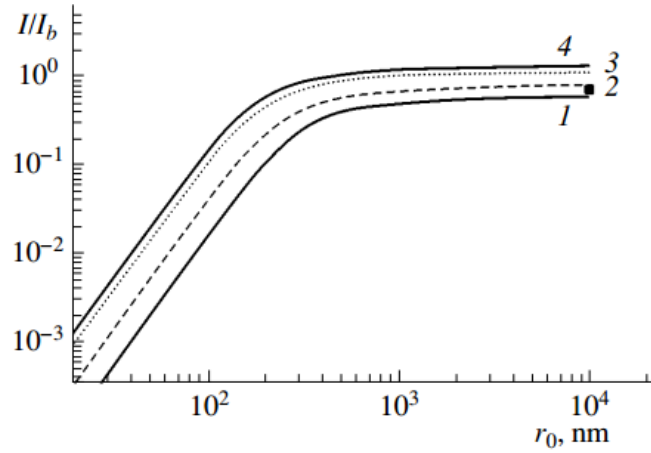


Fig. 5. 4 Normalized emissivity of graphite particles at different temperatures. The emissivity of the particle increases as the size increases [15].

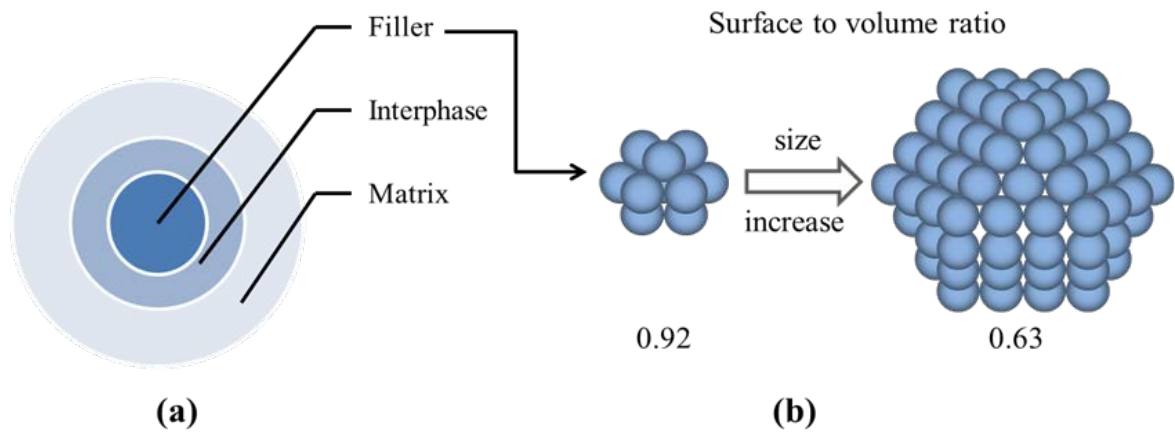


Fig. 5.5 (a) Schematic drawing of polymer-filler composites consisting of polymer matrix, interphase region and filler. (b) Illustration of the change of surface-to-volume ratio as a function of filler size. The surface to volume ratio for a filler is defined as the proportion of surface atoms to total atoms.

Previously, it was believed that nano-filler polymer composites were suitable for radiation cooling materials. However, our experimental observations reported here demonstrate

that there is insignificant temperature difference when a filler size changes from nanometers to micrometers, indicating that cooling effect of coatings is not filler size-sensitive. Our results provide a new reference for material design that has important implications for radiation cooling coatings. The reduced need for filler size control of composite coatings would give coatings wider versatility for industrial and residential applications.

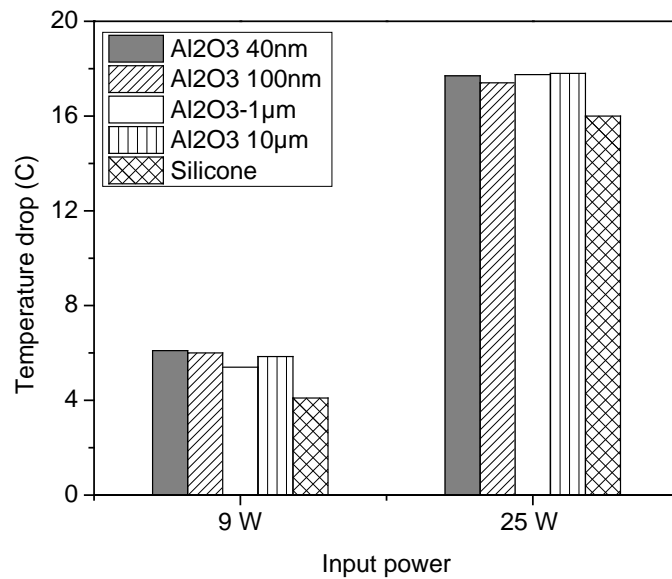


Fig. 5. 6 Reduction of board temperature of Al<sub>2</sub>O<sub>3</sub> composites coatings at input power of 9 W and 25 W. The filler volume fraction is 0.1 and the coating thickness is 70±5 microns.

Figure 5.6 shows the surface temperature reduction of silicone-Al<sub>2</sub>O<sub>3</sub> coating specimens as a function of filler size at two input powers. The silicone-Al<sub>2</sub>O<sub>3</sub> coatings have a filler volume fraction of 0.1 and a thickness of 70±5 microns. Using coatings consisting of Al<sub>2</sub>O<sub>3</sub> fillers, the average board temperature was reduced by 5.8 and 17.7 °C at input power of 9 W and 25 W,



respectively. We can predict that the cooling effects of the coatings will become more obvious at higher input powers.

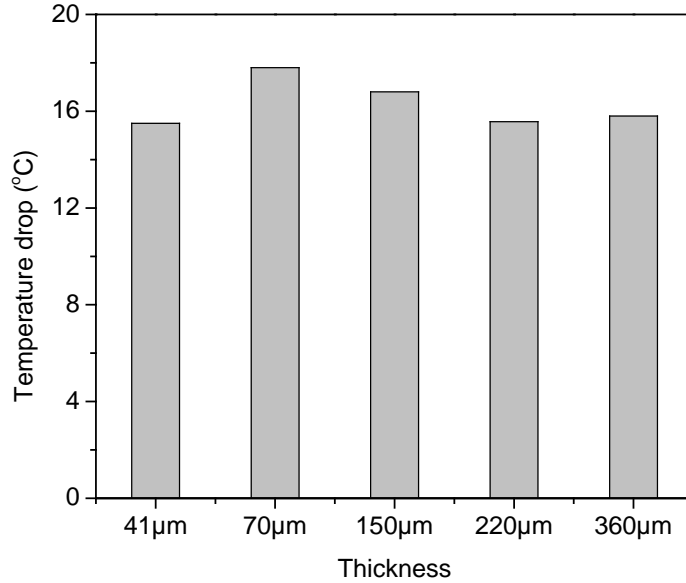


Fig. 5. 7 Illustrates the effect of coating thickness on the cooling effect of  $\text{Al}_2\text{O}_3$  composite coating at input power of 25 W. The filler used is  $1 \mu\text{m}$   $\text{Al}_2\text{O}_3$  powders and the filler volume fraction is 0.1.

The trends of the cooling effect exhibit a thickness dependence for  $\text{Al}_2\text{O}_3$  composite coatings, and that this thickness dependence is non-monotonic. The reduction of board temperature first increases as the thickness increases from 40 nm reaches its peak value at 70 microns, and then gradually decreases as the thickness continues to increase. The board temperature was reduced by 15.5, 17.8, 16.8, 15.6 and 16.2 °C for 40, 70, 150, 200 and 360 μm-thick composite coatings, respectively.

The existence of optimal thickness of coating is attributed by two factors: heat radiation and heat conduction. The emissivity is 0.15 for Al plate and 0.90-0.95 for silicone composites

filled with inorganic filler. The radiation emissivity of composite coating increases as the coating becomes thicker. The high emissivity of the silicone composites effectively enhanced the contribution of radiation to heat transfer. However, since the thermal conductivity of silicone composites is much lower than that of Al plate, the thick composite coating act as thermal barrier with high heat resistance, preventing the heat generated in the system being conducted to the coating surface quickly and efficiently. The first factor dominates when the coating thickness is less than 70 microns, while the second factor overwhelms with further increase in coating thickness. Therefore, determination of the critical optimal thickness of coating is essential to improve the cooling effect of silicone composite coatings.

#### **4.4. Conclusion**

In this study, the cooling effect of silicone composite coatings was investigated through a series of experiments performed on Al substrates. Our experimental results demonstrated for the first time that the filler size of inorganic fillers has insignificant influence on apparent cooling effect of a coating. The application of silicone, Al<sub>2</sub>O<sub>3</sub>, TiO<sub>2</sub> and ZnO composite coatings, the board temperature was reduced from 101.4 °C to 98.3, 96, 97 and 97.3 °C, respectively. The cooling effect is dependent on coating thickness, and that this dependence is non-monotonic. The reduction of board temperature first increases as the thickness increases from 40 nm reaches its peak value at 70 microns, and then gradually decreases as the thickness continues to increase. The present results provide a new reference for material designs, and would give composite coatings wider versatility for industrial and residential applications.

## References

- [1] C. N. Suryawanshi, T. Kim and C. T. Lin, "An instrument for evaluation of performance of heat dissipative coatings." *Rev. Sci. Instrum.*, **81** 035105 (2010)
- [2] M. Mauer, P. Kalenda, M. Honner and P. Vacikova, "Composite fillers and their influence on emissivity." *J. Phys. Chem. Solids*, **73** 1550–1555 (2012)
- [3] A. P. Raman, M. A. Anoma, L. Zhu, E. Rephaeli, and S. Fan, "Passive radiative cooling below ambient air temperature under direct sunlight." *Nature*, **515**(27) 540-544 (2014)
- [4] J. A. Johnson, J. J. Heidenreich, R. A. Mantz, P. M. Baker, and M. S. Donley, "A multiple-scattering model analysis of zinc oxide pigment for spacecraft thermal control coatings" *Prog. Org. Coat.*, **47**(3) 432-442 (2003)
- [5] H. A. Babrekar, N. V. Kulkarni, J. P. Jog, V. L. Mathe and S. V. Bhoraskar, "Influence of filler size and morphology in controlling the thermal emissivity of aluminum/polymer composites for space applications." *Mater. Sci. Eng. B*, **168** 40-44(2010)
- [6] Y.P. Chen, G.Y. Xu, T.C. Guo, N. Zhou, "Infrared emissivity and microwave absorbing property of epoxy-polyurethane/annealed carbonyl iron composites coatings." *Sci. China Technol. Sci.*, **55**(3) 623-628 (2012)
- [7] H. Yu, G. Xu, X. Shen, X. Yan, C. Shao, C. Hu, "Effect of size, shape and floatage of Cu particles on the low infrared emissivity coatings." *Prog. Org. Coat.*, **66** 161-166 (2009)
- [8] M. Baneshi, S. Maruyama, H. Nakai and A. Komiya, "A new approach to optimizing pigmented coatings considering both thermal and aesthetic effects." *J. Quant. Spect. Rad. Trans.*, **110** 152-204 (2009)

- [9] C. N. Suryawanshi and C. T. Lin, "Radiative Cooling: Lattice Quantization and Surface Emissivity in Thin Coatings." *ACS Appl. Mater. Interfaces*, **1** (6) 1334-1338 (2009)
- [10] T. Eyassu, T. J. Hsiao, K. Henderson, T. Kim and C. T. Lin, "Molecular cooling fan: factors for optimization of heat dissipation devices and applications." *Ind. Eng. Chem. Res.*, **53** (50) 19550-19558 (2014)
- [11] Z. W. Wang, Y. M. Wang, Y. Liu, J. L. Xu, L. X. Guo, Y. Zhou, J. H. Ouyang, and J. M. Dai, "Microstructure and infrared emissivity property of coating containing TiO<sub>2</sub> formed on titanium alloy by microarc oxidation." *Curr. Appl. Phys.*, **11** 1405-1409 (2011)
- [12] Y. Mastai, Y. Diamant, S.T. Aruna, and A. Zaban, "TiO<sub>2</sub> nanocrystalline pigmented polyethylene foils for radiative cooling applications: synthesis and characterization." *Langmuir*, **17**, 7118–7123 (2001)
- [13] M. Mauer, P. Kalenda, M. Honner, and P. Vacíková, "Composite fillers and their influence on emissivity." *Phys. Procedia*, **44**, 262–269 (2013)
- [14] S. J. Yu, S. J. Youn and H. Kim, "Size effect of thermal radiation." *Physica B*, 405, 638-641 (2010)
- [15] Yu. V. Martynenko, and L. I. Ognev, "Thermal radiation from nanoparticles." *Tech. Phys.*, **50**(11) 130-132 (2005)
- [16] S. Zhang, X. Y. Cao, Y. M. Ma, Y. C. Ke, J. K. Zhang, and F. S. Wang, "The effects of particle size and content on the thermal conductivity and mechanical properties of Al<sub>2</sub>O<sub>3</sub>/high polyethylene (HDPE) composites." *Express Poly. Lett.* **5**(7), 581 (2011)

# **CHAPTER 6:**

## **DUAL-FUNCTIONAL SILICONE COMPOSITES FOR HIGH OPTICAL DIFFUSE REFLECTANCE AND PASSIVE COOLING**

### **6. 1. Introduction**

Thermal management is a critical issue for high power LEDs, LCD display backlighting and solar cells [1-5]. Passive cooling coatings are very attractive for electronic devices since no additional space or power supply is required. In real engineering applications, the cooling ability of a coating layer is realized by heat dissipation due to radiation, convection and conduction. Thus, the combined cooling effect of heat radiation, conduction and convection is what really matters in engineering applications of a passive device coating material. Recently, the polymer-filler composites have been investigated for passive cooling of electronic systems, cars and buildings [6-10]. The cooling coatings proposed in those studies can effectively reduce the surface temperature of objects if the heat source is solar radiation. However, their effectiveness in cooling the electronic devices is very questionable. There is still a strong need for the development of passive cooling coatings for applications in higher power LEDs and LCD backlight units.

The light management is another important issue in optoelectronic devices [11-15]. The light trapped within the device package needs to be diffused, distributed and guided in order to achieve high conversion efficiency. The reflective materials employed in LEDs and LCD backlights has significant effect on brightness, uniformity, color and stability of the backlight

units and the LCD modules. Conventionally, LED packages are mounted on a PCB in the form of array by surface mount technology and then attached on a heat sink, to manufacture a LED array unit used in a LCD backlight. Such manufacturing process of LED units is complicated and expensive. Besides, the increased overall thickness of LED units is an obstacle to the thinning of LCD backlights. The problem mentioned above can be possibly solved by applying a layer of dual-functional polymer-filler composite coating on the PCB. That is, the composite coating can increase the surface reflection of PCB to improve the brightness and uniformity, due to its high reflectance. Meanwhile, the composite coating can help dissipate the heat from LEDs via radiation to increase the light output and lifetime of LEDs, due to its cooling ability. The elimination of heat sink from the structure of LED units can largely simplify the manufacturing process, save the manufacturing cost and reduce the overall thickness of LED units and, ultimately, backlight units.

However, in view of the significance, both technologically and scientifically, it is surprising to find that there is no report on polymer-filler composite coatings with both optical and thermal properties. In this study, for the first time, we developed a dual-functional optically reflective and thermally cooling composites, and carried out a systematic experimental study to investigate dependence of the light reflectance and apparent cooling effect on filler type, filler size and filler volume fraction of polymer-filler composite coatings. The new materials we developed can be used as diffuse reflector to provide better overall optical aesthetics for displays. Meanwhile, it can be used as passive cooling coatings in advanced general LED lighting, LCD display backlighting, solar cells and other energy related applications.

## **6.2. Experiment**

### 6.2.1 Fabrication of samples

In the experiment, silicone-based diffuse reflective films were fabricated by mixing transparent silicone resin with inorganic fillers. The inorganic fillers used for samples are  $\text{TiO}_2$ , BN (from Sigma-Aldrich) and ZnO (from Inframat Advanced Materials Inc) powders. The properties of materials used in polymer-filler reflectors are listed in Table 6. 1. The samples were prepared according to the technological process as shown in Fig. 6.1. The thickness of coating was measure by coating thickness gauge (CEM Model DT-156).

Table 6. 1. Properties of materials used for samples

Materials	Refractive index ( $\lambda=450$ nm)	Average filler size ( $\mu\text{m}$ )	Volume fraction
Silicone resin	1.41	-	0.975, 0.95, 0.8, 0.7
$\text{TiO}_2$ powers	2.81	1	0.025, 0.05, 0.1, 0.2, 0.3
BN powders	1.81	1	0.025, 0.05, 0.1, 0.2, 0.3
ZnO powders	2.11	1	0.025, 0.05, 0.1, 0.2, 0.3

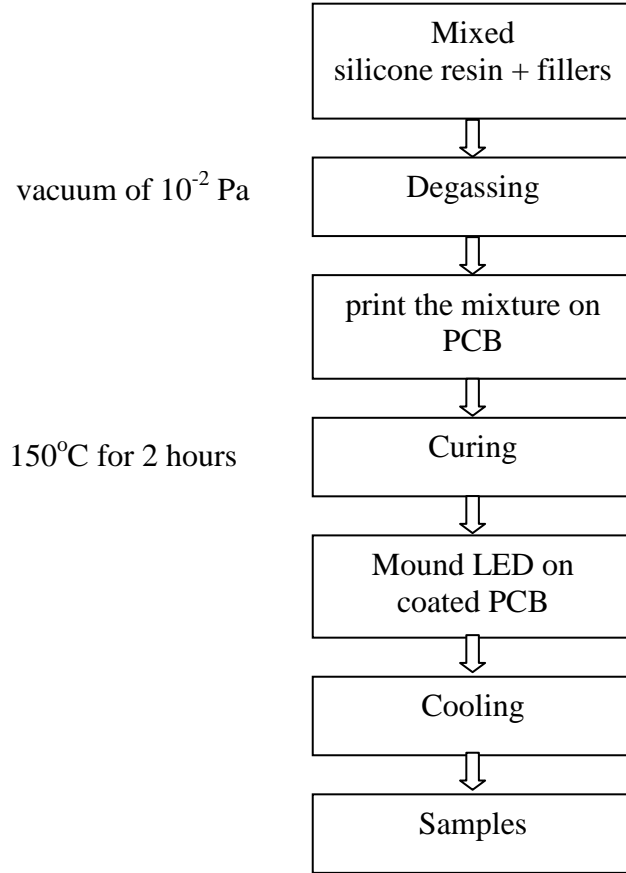


Fig. 6. 1. Technological process for samples preparation.

### 6.2.2 Temperature measurement

The apparent cooling effect is determined by comparing the temperature decrease in LED emitter of the coated LED unit with respect to the baseline (LED mounted on uncoated PCB) by following the same reported experimental set up and procedure. The main part of the LED unit consists of a LED package on a PCB, the schematic of which is shown in Fig. 6.2. The sample was heated by turning on a 10 W LED light for 30 minutes. A good thermal contact was formed between the LED emitter and PCB by soldering. The whole heating system is set up inside a



glass shield without forced air flow. The ambient temperature is kept at 23 °C. The surface temperature of the LED emitter is directly measured by thermometer (Omega, model CL3515R).

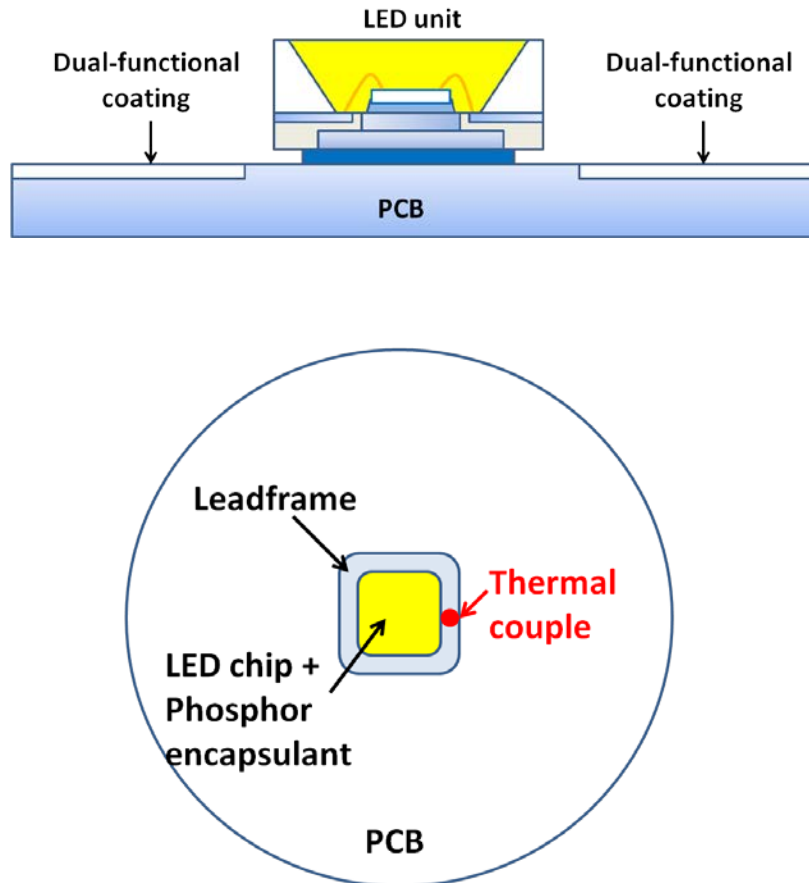


Fig.6.2 Cross-sectional and top-view structure of LED unit consist of a LED package mounted on a coated PCB. Red spot is the measurement position for LED emitter temperature.

### 6.2.3 Light reflectance measurement

The light reflectance of the fabricated samples at a wavelength range from 400 to 800 nm was measured using a conventional light reflectometer (Filmetrics Model F20).

### 6. 3. Result and discussion

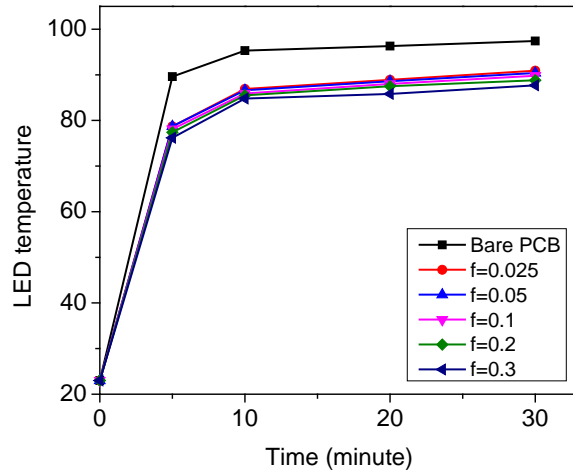
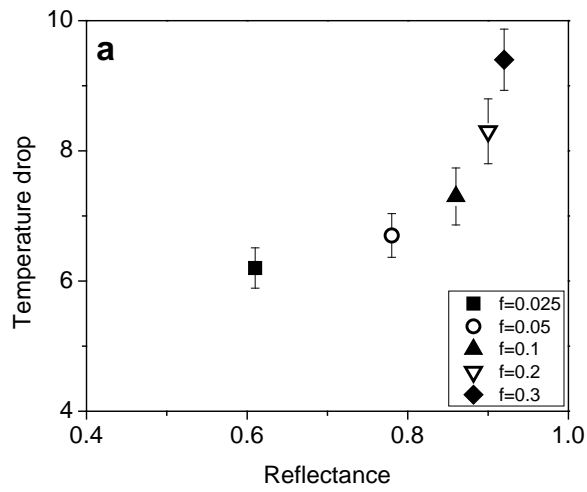


Fig. 6.3 Temperature vs. time for LED unit incorporated with ZnO-silicone composite coatings with different filler volume fraction.



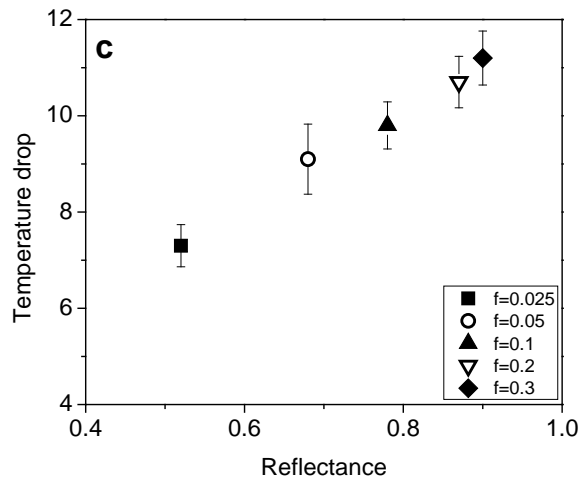
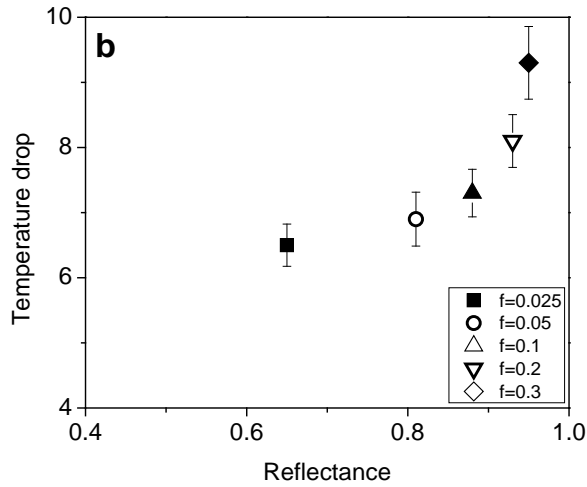


Fig. 6.4 Temperature reduction of LED unit consist of LED emitter and PCB coated with (a) ZnO, (b) TiO<sub>2</sub> and (c) BN filled silicone composites vs. light reflectance of silicone composite coatings. The filler volume fractions are 0.025, 0.05, 0.1, 0.2 and 0.3. The coating thickness is 50±5 microns. The power of LED is 10 Watts.

Figure 6.3 presents the temperature of LED emitter against time. The filler used in composite coating is ZnO powders. The plot shows the LED emitter has lower temperature rise if the PCB was coated with composite cooling coatings. Figure 6.4 show the relationship between filler volume fraction in silicone composites, and the temperature reduction of a LED unit consist of LED emitter and PCB coated with silicone composite coatings filled with ZnO, TiO<sub>2</sub> and BN fillers. The temperature drop of LED is defined as the difference of LED emitter temperature

between LED units with and without coating on PCBs. As indicated in plots a, b and c, by increasing the filler volume fraction, the temperature of LED unit experience a gradual decrease. For LED unit with ZnO and TiO<sub>2</sub> filled silicone composite coatings, the reduction in temperature is slow as the filler volume fraction increases from 0.025 to 0.1, then the reduction becomes rapid as the filler volume fraction further increases from 0.1 to 0.3. The addition of fillers into silicone resin coatings improves heat dissipation by reducing the temperature of LED by 9.3 °C, 9.2 °C, and 11.4 °C for ZnO, TiO<sub>2</sub> and BN fillers, respectively.

Two contributions need to be taken into account during the increase of filler volume fraction: heat radiation and heat conduction. (1). Heat radiation: the emissivity is 0.15 for Al substrate, 0.65 for pure silicone resin and 0.90-0.95 for silicone composites filled with inorganic fillers. The radiation emissivity of composite coating gradually increases as the filler volume fraction increases. The high emissivity of the silicone composites effectively enhanced the contribution of radiation to heat transfer. (2). Heat conduction: the thermal conductivity of silicone resin, ZnO filler, and TiO<sub>2</sub> filler and BN filler is 0.18 W/m·K, 37 W/m·K, 11.8 W/m·K and 30-600 W/m·K, respectively. Since the thermal conductivity of pure silicone resin is much lower than those of inorganic fillers, the pure silicone coating act as thermal barrier with high heat resistance, preventing the heat generated in the system being conducted to the coating surface quickly and efficiently. The dispersed filler particles act as spots of lower thermal resistance microscopically. With an increase in filler volume fraction, heat tends to dissipate along the low-thermal-resistance channels consisting of clusters of micro-particle fillers. Therefore, an increase in the filler volume fraction is essential to improve the apparent cooling effect of silicone composite coatings.

The variation in light reflectance with the filler volume fraction for silicone composite coatings filled with ZnO, TiO<sub>2</sub> and BN fillers, is also shown in figure 6. 3. With a given thickness of 50 micrometers, the light reflectance first rapidly increases as the volume fraction increases from 0.025 to a critical value around 0.2, and then increases slowly as the volume fraction continues to increase. The plots indicate that the critical volume fractions for ZnO, TiO<sub>2</sub> and BN fillers to achieve a 90% reflectance at 450nm wavelength are 0.2, 0.2 and 0.3, respectively. The common commercial PCB white coating has a reflectance of 70-80% at visible light wavelength. Our silicone composite coating, with a filler volume fraction higher than 0.3, can provide a higher reflectance to reduce the light loss, increase light output, improve the brightness, uniformity, color and stability. Meanwhile, the high volume fraction of filler offers silicone composite coating a good passive cooling ability to reduce the heat load to LEDs and LCD backlight units, increase the energy efficiency and extend the operation lifetime. Furthermore, the utilization of dual-functional silicone composite coatings as alternative reflectors and heat dissipation layers, can eliminate the need of heat sink from the structure of LED units, thus largely simplifying the manufacturing process, lowering the manufacturing cost and reducing the overall thickness of LED units and, ultimately, backlight units.

#### **6. 4. Conclusion**

In this study, for the first time, we developed a dual-functional optically reflective and thermally cooling composites, and carried out a systematic experimental study to investigate the dependence of the light reflectance and apparent cooling effect on filler type, filler size and filler volume fraction of polymer-filler composite coatings. Our experimental results demonstrated for the first time that the apparent cooling effect and light reflectance of a coating is strongly

dependent on filler volume fraction. The apparent cooling effect first increases slowly as the filler volume fraction increases from 0.025 to 0.1, and then rapidly increases as the filler volume fraction continues to increase to 0.3. The silicone composite coatings improves heat dissipation by reducing the temperature of LED by 9.3 °C, 9.2 °C, and 11.4 °C with addition of ZnO, TiO<sub>2</sub> and BN fillers, respectively. It was demonstrated that the addition of inorganic fillers to a volume fraction higher than 0.2 can effectively improve the apparent cooling effect and light reflectance of silicone composites. The present study provides a new material which can be used in advanced general LED lighting, LCD display backlighting, solar cells and other energy related applications.

## References

1. Y. Taguchi, and J. Sawada, "White heat-curable silicone resin composition and optoelectronic part case." U.S. Patent 8173053 B2, 2013
2. J. Mozzochette, and E. Amaya, "Light emitting diode arrays with improved light extraction." U.S. Patent 0225222 A1, 2005
3. E. Moulin, U. W. Paetzold, H. Siekmann, J. Worbs, A. Bauer, and R. Carius, "Study of thin-film silicon solar cell back reflectors and potential of detached reflectors." Energy Procedia. Vol.10, 106-110 (2011)
4. M. D. Kempe, M. Kilkenny, T.J. Moricone, J.Z. Zhang, "Accelerated stress testing of hydrocarbon-based encapsulants for medium-concentration CPV applicaitons." in Proc. 34th IEEE PVSC, Philadelphia, 1826-1830 (2009)
5. B. L. Ahn, J. W. Park, S. Yoo, J. Kim, S.B. Leigh and C. Y. Jang, "Saving in cooling energy with a thermal management system for LED lighting in office buildings" Energies vol. 8, 6658-6671 (2015)
6. A. P. Raman, M. A. Anoma, L. Zhu, E. Rephaeli, and S. Fan, "Passive radiative cooling below ambient air temperature under direct sunlight." Nature, **515**(27) 540-544 (2014)
7. J. A. Johnson, J. J. Heidenreich, R. A. Mantz, P. M. Baker, and M. S. Donley, "A multiple-scattering model analysis of zinc oxide pigment for spacecraft thermal control coatings" Prog. Org. Coat., **47**(3) 432-442 (2003)
8. C. N. Suryawanshi and C. T. Lin, "Radiative Cooling: Lattice Quantization and Surface Emissivity in Thin Coatings." ACS Appl. Mater. Interfaces, **1** (6) 1334-1338 (2009)

9. H. A. Babrekar, N. V. Kulkarni, J. P. Jog, V. L. Mathe and S. V. Bhoraskar, "Influence of filler size and morphology in controlling the thermal emissivity of aluminum/polymer composites for space applications." *Mater. Sci. Eng. B*, **168** 40-44(2010)
10. H. Gao, H. Chen, X. Zhang, P. Zhang, J. Liu, H. Liu and Y. Cui, "High-performance GaN-based light-emitting diodes on patterned sapphire substrate with a novel hybrid Ag mirror and atomic layer deposition-TiO<sub>2</sub>/Al<sub>2</sub>O<sub>3</sub> distributed Bragg reflector backside reflector" *Opt. Eng.*, vol. 52, 2013, 063402
11. A. Lin, Y. K. Zhong, S. M. Fu, C. W. Tseng, and S. L. Yan, "Aperiodic and randomized dielectric mirrors: alternatives to metallic back reflectors for solar cells" *Opt. Express* 22, A880 (2014)
12. O. Berger, D. Inns, and A. G. Aberle, "Commercial white paint as back surface reflector for thin-film solar cells" *Sol. Energy Mater. Sol. Cells* 91, 1215 (2007)
13. C. Pan, C. Su, H. Cheng, and C. Pan, "Backlight module and brightness enhancement film thereof" US 7290919 B2 (2007)
14. W. G. O'Brien, "Diffuse reflector, diffuse reflective article, optical display, and method for producing a diffuse reflector." US 20100014164 A1



## **CHAPTER 7:**

### **SUMMARY AND CONCLUSIONS**

The increasing market share of optoelectronic devices such as LEDs and its applications is driven by the rapid progress in LED technologies and the energy saving demands. Continuous innovation and improvement of packaging materials have been introduced to improve the devices overall conversion efficiency.

The first chapter briefly introduces the basic concepts and challenges of LEDs. LEDs are continuously replacing the conventional light sources due to its superior energy conversion efficiency, lifetime and reliability. However, optical and thermal management are two important issues for LEDs and its application in general lighting and LCD backlight displays. More efforts are needed in developing packaging materials to enhance the optical and thermal performance of devices.

In chapter 2, the effect of filler size on light reflectance of polymer-filler composite reflectors has been studied. An analytical model was developed and utilized to investigate the critical sizes of inorganic fillers required to obtain the highest reflectance. Our results demonstrate for the first time that for different inorganic fillers, a critical filler size that ranges from one submicron to several microns provides the maximum reflectance for polymer-based reflectors. The critical size for fillers to effectively reflect incident radiation at 450nm wavelength is around 0.8 microns for Al<sub>2</sub>O<sub>3</sub> pigments, and 0.2 microns for TiO<sub>2</sub> pigments. The developed analytical model has been experimentally verified as an effective method to optimize polymer-filler composite reflectors.

In chapter 3, the critical thickness at which the reflectance of composite reflector reaches its saturation value is investigated. An analytical model was modified to effectively predict the critical parameters for polymer-filler composite reflectors on various substrates. It was demonstrated the critical thickness is dependent on back reflection of the substrate, filler volume fraction, filler size, as well as the matrix-filler refractive indices difference. For BN-silicone reflectors, the critical thickness at which the reflectance becomes stable is around 200  $\mu\text{m}$  for BN-silicone reflectors, and around 100  $\mu\text{m}$  for ZnO-silicone reflectors. The results provide an empirical basis for selecting thickness and filler volume fraction to produce cost-effective polymer-based diffuse reflectors.

In chapter 4, silicone based reflectors were optimized to obtain high reflectance ( $>0.9$ ) with a reduced thickness (less than 200  $\mu\text{m}$ ) for backlights application. The filler-dependent thermal stability of silicone composite reflectors were investigated. Silicone reflective films filled with  $\text{Al}_2\text{O}_3$  show the best stability, while silicone reflective films filled with  $\text{SiO}_2$  show the worst. The filler-dependent high temperature and moisture stability of silicone composite reflectors were also investigated. Silicone reflective films filled with ZnO show the best stability, while silicone reflective films filled with  $\text{SiO}_2$  show the worst. Our results provide an important guidance for the development of highly reflective and inexpensive thin reflective films for backlight units application.

Chapter 5 studies the passive radiative cooling coatings and their apparent cooling effect on electronic devices. It is demonstrated for the first time that the filler size of inorganic fillers has insignificant influence on apparent cooling effect of a coating. The application of silicone,  $\text{Al}_2\text{O}_3$ ,  $\text{TiO}_2$  and ZnO composite coatings, the board temperature was reduced from 101.4  $^\circ\text{C}$  to 98.3, 96, 97.5 and 97  $^\circ\text{C}$ , respectively. The apparent cooling effect showed a slight dependence

on coating thickness, and that this dependence is non-monotonic. The reduction of board temperature first increases as the thickness increases from 40 nm reaches its peak value at 70 microns, and then gradual decreases as the thickness continues to increase. Our results provide a new reference for material designs, and would give composite coatings wider versatility by eliminating the size control.

In chapter 6, a new class of dual-functional composites with optical reflectance and passive cooling ability was developed for optoelectronic device applications. We have demonstrated for the first time that the apparent cooling effect and light reflectance of coating is strongly dependent on filler volume fraction. The apparent cooling effect experience a rapid increase as the filler volume fraction higher than 0.1 for common white inorganic fillers. Our result showed that silicone composite coatings successfully reduced the temperature of LED by 9.3 °C, 9.2 °C, and 11.4 °C with addition of ZnO, TiO<sub>2</sub> and BN fillers, respectively. It was demonstrated the addition of inorganic fillers to a volume fraction higher than 0.2 can effectively improve the apparent cooling effect and light reflectance of silicone composites. The use of dual-functional composites is expected to eliminate heat sink from LED units leading to a simplified manufacturing process, lower manufacturing cost and reduced overall thickness of LED units and, ultimately, backlight units.